

**AN INVESTIGATION INTO THE ELECTRO-ACOUSTIC
RESPONSE CHARACTERISTICS OF SEVERAL MIXTURES
OF THE TITANATES OF BARIUM, CALCIUM AND LEAD**

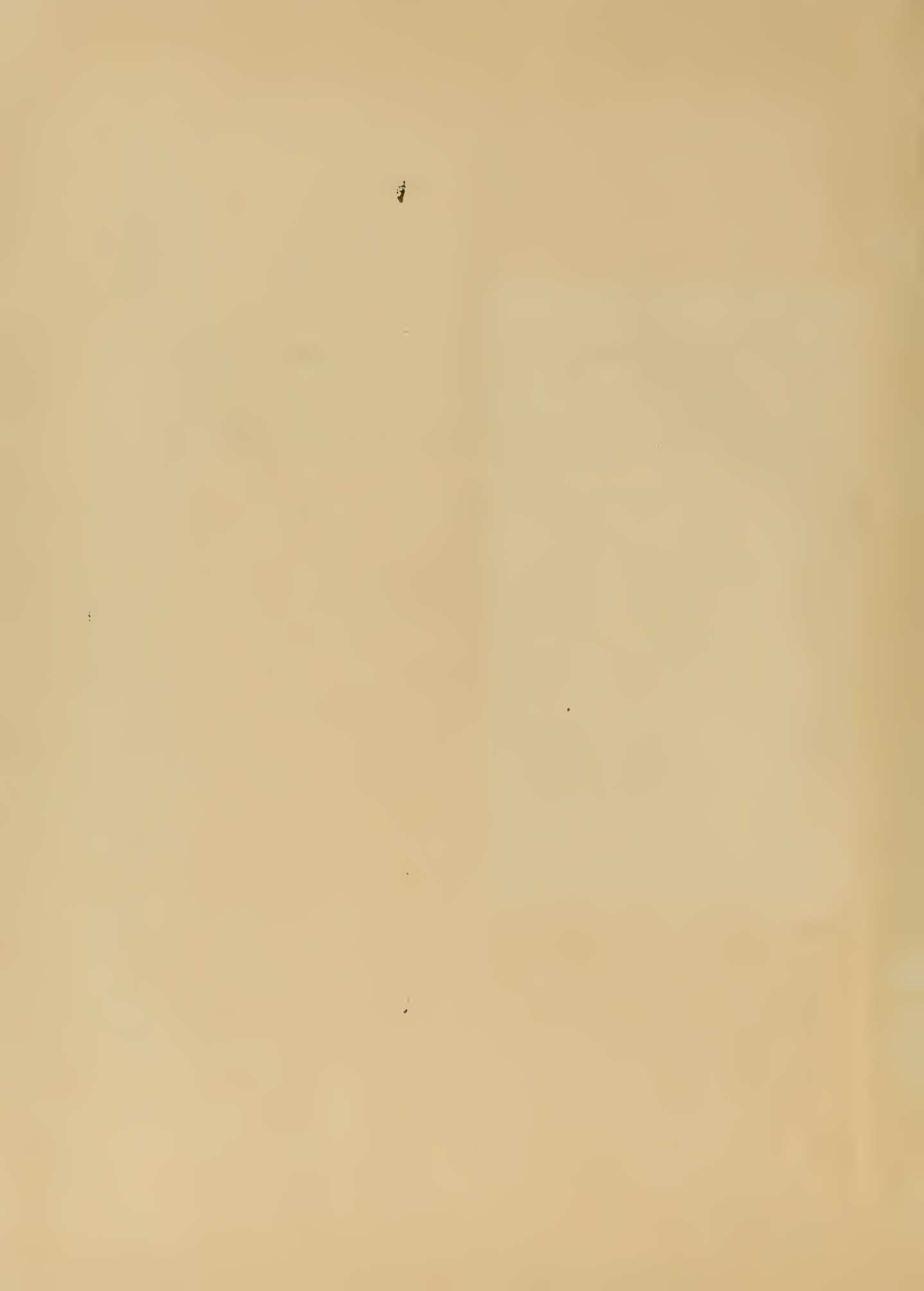
William Francis Clifford, Jr.

LIBRARY
U.S. NAVAL POSTGRADUATE SCHOOL
MONTEREY, CALIFORNIA

LIBRARY
U.S. NAVAL POSTGRADUATE SCHOOL
MONTEREY, CALIFORNIA

AN INVESTIGATION INTO THE ELECTRO-ACOUSTIC
RESPONSE CHARACTERISTICS OF SEVERAL MIXTURES
OF THE TITANATES OF BARIUM, CALCIUM AND LEAD

William F. Clifford, Jr.



8854

CLIFFORD

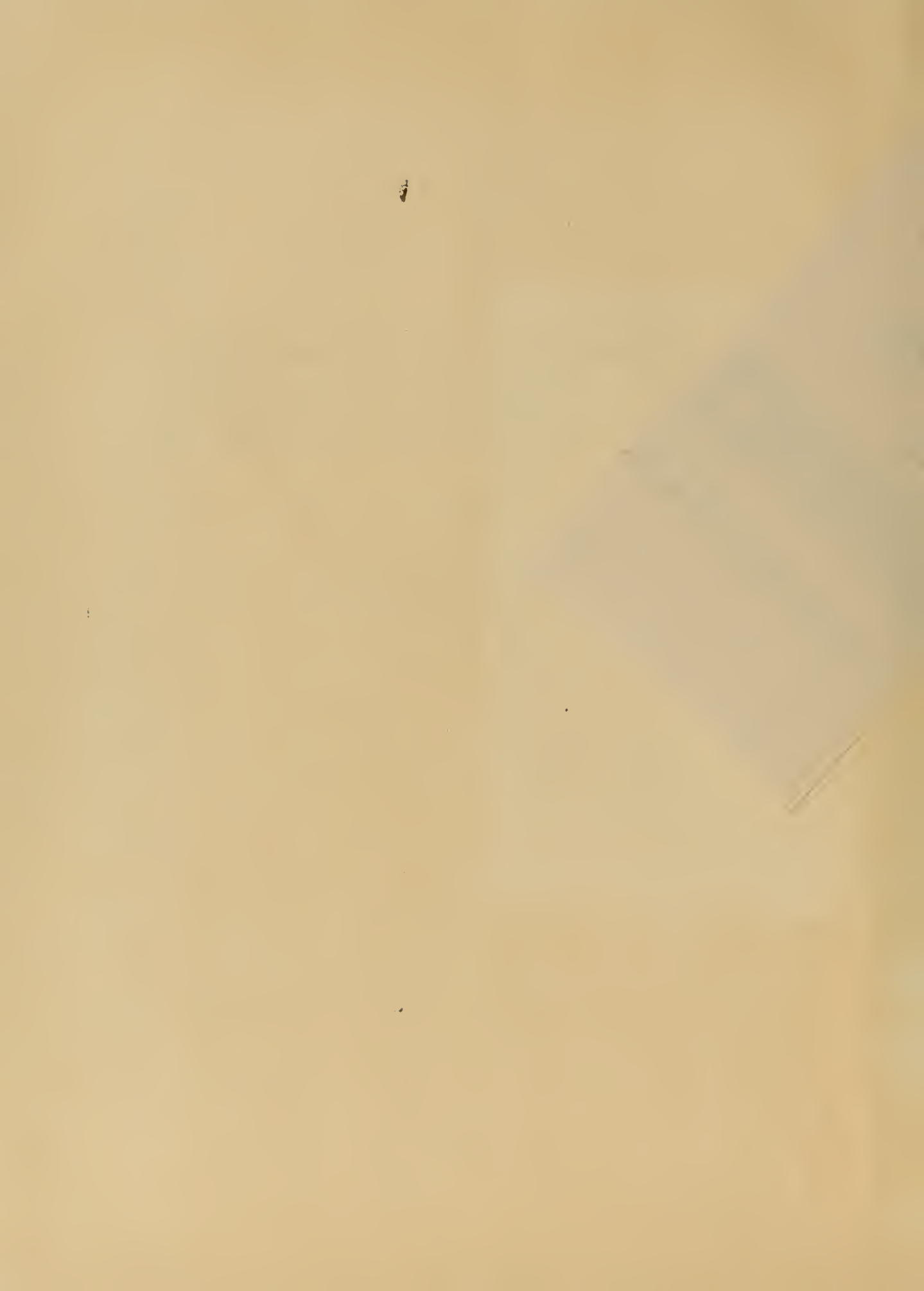
1956

THESIS
C512

Letter on cover:

AN INVESTIGATION TO THE ELECTRO-
ACOUSTIC RESPONSE CHARACTERISTICS
OF SEVERAL MIXTURES OF THE
TITANATES OF BARIUM, CALCIUM AND
LEAD

William Francis Clifford, Jr.



AN INVESTIGATION INTO THE ELECTRO-ACOUSTIC
RESPONSE CHARACTERISTICS OF SEVERAL MIXTURES
OF THE TITANATES OF BARIUM, CALCIUM AND LEAD

by

William Francis Clifford, Jr.
Lieutenant, United States Navy

Submitted in partial fulfillment
of the requirements
for the degree of
MASTER OF SCIENCE
IN
ENGINEERING ELECTRONICS

United States Naval Postgraduate School
Monterey, California

1 9 5 6

Thesis
C512

This work is accepted as fulfilling
the thesis requirements for the degree of

MASTER OF SCIENCE
IN
ENGINEERING ELECTRONICS

from the
United States Naval Postgraduate School

PREFACE

The work described herein was originated and completed during the period 3 January to 16 March 1956 during the writer's ten week industrial experience tour at Pacific Division, Bendix Aviation Corporation, North Hollywood, California. Appreciation is gratefully acknowledged for the many helpful discussions with engineers in the transducer and ceramic laboratories. These were a large help in the manufacture of the test elements and completion of the measurements.

TABLE OF CONTENTS

	Page
CERTIFICATE OF APPROVAL	i
PREFACE	ii
TABLE OF CONTENTS	iii
LIST OF ILLUSTRATIONS	iv
SYMBOLS AND ABBREVIATIONS	vi
CHAPTER	
I INTRODUCTION	1
II FUNDAMENTAL PROPERTIES OF BARIUM TITANATE	5
1. General	5
2. Cell Structure of Barium Titanate	13
3. Permanent Polarization	14
4. Hysteresis in Ferroelectrics	15
5. Additives to Barium Titanate Elements	19
6. Comparison of Common Piezoelectric Materials	20
III ANALYSIS OF AN ELECTROMECHANICAL NETWORK	26
1. Transduction Coefficient	26
2. Motional Impedance	27
3. Efficiency	32
4. Electromechanical Coupling Coefficient	33
IV EXPERIMENTAL WORK	41
1. Preparation of Test Samples	41
2. Philosophy of Measurements	43
3. Total Impedance Circles and Efficiency at Resonance	43
4. Variation of Input Impedance with Temperature	46
5. Electromechanical Coupling Coefficient	51
6. Hysteresis Curves	51
V CONCLUSIONS	58
BIBLIOGRAPHY	63
APPENDIX I DIELECTRIC PROPERTIES OF CERAMIC MIXES	66

LIST OF ILLUSTRATIONS

Figure	Page
1. Dielectric Constant of Barium Titanate (Mix 1) versus Temperature	6
2. Dielectric Constant of Mix 2 versus Temperature . .	7
3. Dielectric Constant of Mix 3 versus Temperature . .	8
4. Dielectric Constant of Mix 4 versus Temperature . .	9
5. Dielectric Constant of Mix 5 versus Temperature . .	10
6. Dielectric Constant of Mix 6 versus Temperature . .	11
7. Dielectric Constant of Mix 7 versus Temperature . .	12
8. Structure of a Barium Titanate Cell	13
9. Typical Hysteresis Loop of a Ferroelectric Material	17
10. Circuit for Observation of Hysteresis Loop	18
11. Equivalent Circuit for a Hydrophone	22
12. Several Modes of Operation of a Ceramic Element . .	24
13. General Equivalent Circuit for an Electromechanical Transducer	26
14. Motional Impedance Circle of an Electromechanical Transducer	31
15. Electrical Equivalent Circuit for an Electromechanical Transducer near Resonance	34
16. Impedance Circles in Air, Mix 1 through 3	36
17. Impedance Circles in Air, Mix 4 through 7	37
18. Impedance Circles in Water, Mix 1 through 3	38
19. Impedance Circles in Water, Mix 4 through 7	39
20. A Typical Firing Cycle	40

Figure		Page
21.	Normalized Efficiency at Resonance, Mix 1 through 7 . .	45
22.	Equivalent Circuit for Computing Power Variations . . .	47
23.	Input Resistance versus Temperature, Mix 1 through 7 .	49
24.	Input Reactance versus Temperature, Mix 1 through 7 . .	50
25.	Power Loss versus Temperature, Mix 1 through 7	52
26.	Electromechanical Coupling Coefficient, Mix 1 through 7	53
27.	Hysteresis Loops, Mix 1 through 8	55
28.	Dielectric Constant versus Temperature, Mix 8 - 11 . .	67
29.	Dielectric Constant at Room Temperature versus Mix . .	69

TABLE

I.	Comparison of Common Piezoelectric Materials	21
II.	Composition of Mixes Tested	41
III.	Summary of Data	59

SYMBOLS AND ABBREVIATIONS

P_e	electronic and atomic electric polarization
P_d	electric polarization due to dipole moment in ferro-electric crystals
P	total electric polarization
η	electric susceptibility
D	electric displacement
E	electric field strength; echo level in decibels re 1 dyne/cm ²
K	permittivity
T	stress
S	strain; source level in decibels re 1 dyne/cm ²
g	piezoelectric coefficient, ratio of open circuit voltage to applied force
d	piezoelectric coefficient, ratio of strain to applied field
k	electromechanical coupling coefficient
Z_e	electrical input impedance to a clamped element
z_m	mechanical impedance of vibrating element
T_{em}	transduction coefficient relating electrical effect upon input due to mechanical motion
T_{me}	transduction coefficient relating mechanical effect upon vibrating element due to electric current flow
T	target strength in decibels
Z_{in}	total electrical input impedance of ceramic element
Z_L	mechanical load impedance of medium
Z_{mot}	component of input electric impedance due to motion

$\text{Im}(\quad)$ imaginary part of (\quad)

$\text{Re}(\quad)$ real part of (\quad)

η_{res} efficiency at resonance

a absorption coefficient of water in decibels per yard

A transmission anomaly in decibels

CHAPTER I

INTRODUCTION

The use of electro-mechanical transducers for producing high intensity sonic and ultrasonic waves has been a most important device in the field of pro and anti-submarine warfare since Langevin's work near the conclusion of the first World War. This important military use, coupled with the use of ultrasonics as a research tool in investigating the properties of liquids and gases and more recently as an industrial device for flaw detection in metals, sonic and ultrasonic cleaning techniques, and the treatment and mixing of certain liquids, has made the discovery of new electro-mechanical transducing materials an important event in the aforementioned military, research and industrial fields. Electro-mechanical transduction to sonic and ultrasonic outputs at high power levels depends primarily upon the magnetostrictive, piezoelectric and electrostrictive effects.

Joule is generally credited with the discovery of the magnetostrictive effect in the mid-nineteenth century although some manifestations of this effect had been observed previously. Magnetostriction is the phenomenon whereby certain metals exhibit a change in dimension when subjected to a magnetic field. The change in dimension is independent of the direction of the applied magnetic field, and may be

either an expansion or a contraction depending upon the material used.

In the late nineteenth century, the piezoelectric effect (that is, the phenomenon whereby an applied mechanical stress produces an electric polarization in a body) was discovered in certain natural crystals by the Curie brothers. Within a year the reverse effect, that an applied electric field can produce a stress and a resulting strain or deformation, was predicted by Lippmann and experimentally verified by the Curies. These early discoveries of the piezoelectric effect have been followed by the observation of the effect in a multitude of crystalline materials, and a great amount of quantitative data has resulted from a systematic study conducted at the Bell Telephone Laboratories since the early 1940's⁽¹⁷⁾. In the true piezoelectric effect, the strain is a single-valued function of the applied field; that is, a reversal in the polarity of the applied field will produce a reversal in the sign of the resulting strain.

The electrostrictive effect, or the stress occurring in a dielectric between two conducting electrodes at different potentials, is common to all dielectric materials although the effect is small except in ferroelectric materials such as Rochelle Salt and certain ceramics. These ferroelectric materials derive their name from the very close similarity observed between the electrical effects in these bodies and the magnetic behavior of the ferrites. The electrostrictive ef-

fect in ferroelectric materials is generally of two types, that appearing in Rochelle Salt (often called a quadratic piezoelectric effect) where the strain is proportional to the product of the spontaneous polarization and the applied electric displacement, and that appearing in certain ceramics where the strain is proportional to the square of the applied field and is in every way analogous to the magnetostrictive effect in a ferromagnetic material as already mentioned briefly⁽¹⁷⁾.

The aforementioned ferroelectric ceramics include a large number of members of the families of compounds known as titanates, niobates and metaniobates, including those compounds of lead, calcium, barium, cobalt, strontium and many others. These constitute the newest electromechanical transducing materials to find wide application in military and industrial uses.

This paper will report the results of an investigation conducted into the effect upon some characteristics of barium titanate ceramic transduction elements due to the addition of small percentages of the titanates of calcium and lead. The characteristics chosen are those that pertain directly to the suitability of these ceramic mixtures for use in underwater electro-acoustic transducers (the primary use of which is in military sonar equipments). These characteristics include (1) the efficiency at mechanical resonance, a measure of the efficiency of conversion of electrical energy to acoustic

energy; (2) the electro-mechanical coupling coefficient, a measure of the electrical energy converted into mechanical energy; and, (3) the variation of input impedance with temperature. The latter characteristic is analyzed by computing the loss of power delivered to the transducer by a matched driver stage with the aid of a hypothetically assumed situation.

CHAPTER II

FUNDAMENTAL PROPERTIES OF BARIUM TITANATE

1. General

Investigation into the dielectric properties of titanium dioxide was spurred by the mica shortage experienced during World War II. These investigations led to further study of the dielectric properties of compounds of titanium dioxide with oxides of certain elements such as barium, calcium, lead, bismuth, etc. These compounds, known as titanates, exhibited several interesting properties, among them an extremely high dielectric constant and a strong dependence of this dielectric constant upon temperature and an applied d-c bias. It was through investigation of this dependence upon the bias field that the piezoelectric effect in barium titanate was discovered⁽⁷⁾.

Barium titanate is a member of a class of crystals including Rochelle Salt (RS) and potassium dihydrogen phosphate (KDP) exhibiting ferroelectric properties. Such materials exhibit a spontaneous polarization in one or more directions of the crystal axes over a definite temperature range. The phenomena associated with this effect include a polarization-field curve in the form of a hysteresis loop (similar to familiar B-H curves for magnetostrictive elements), a mechanical strain-electric field curve in a hysteresis loop, and a wide



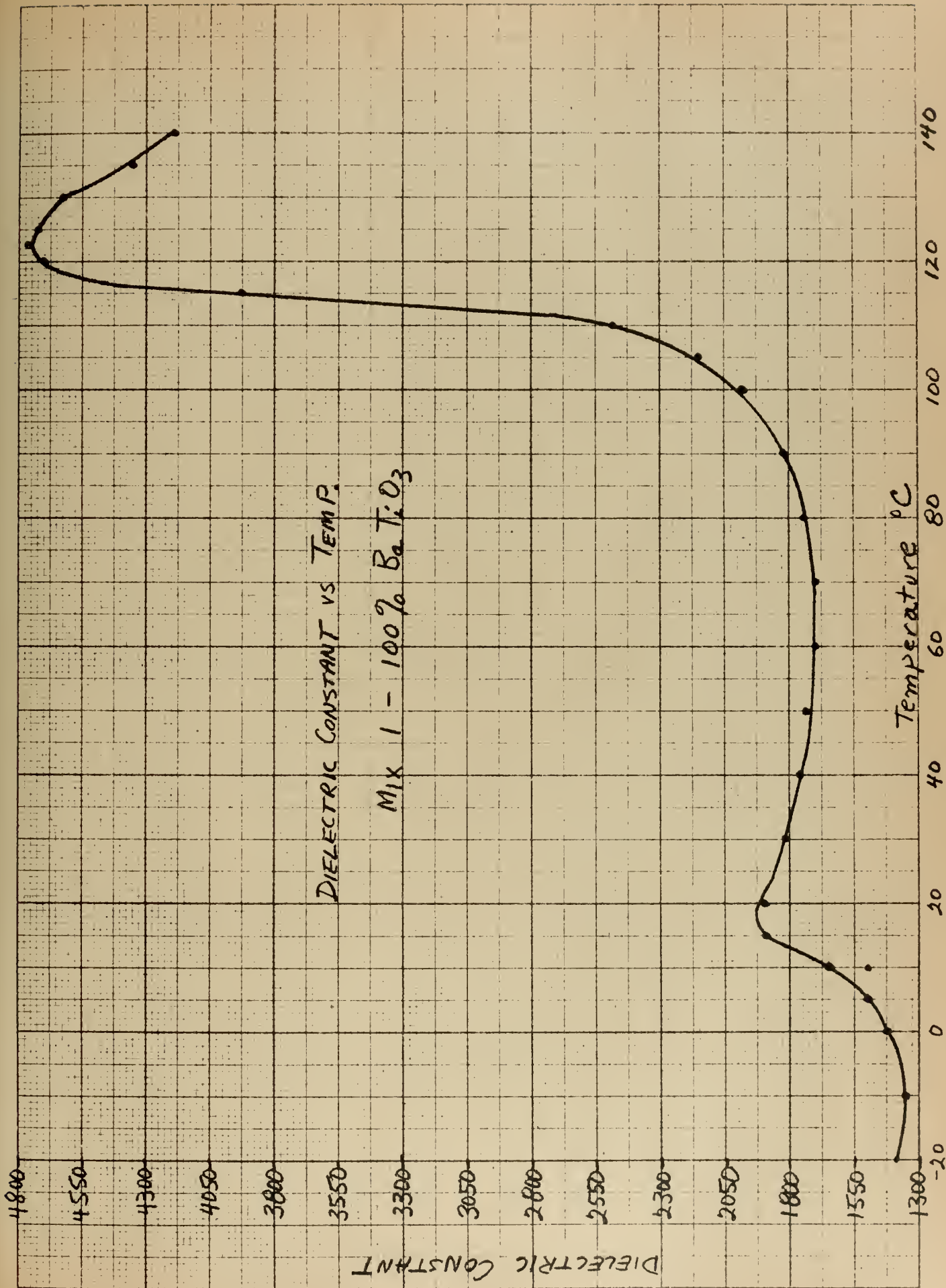


FIGURE 1

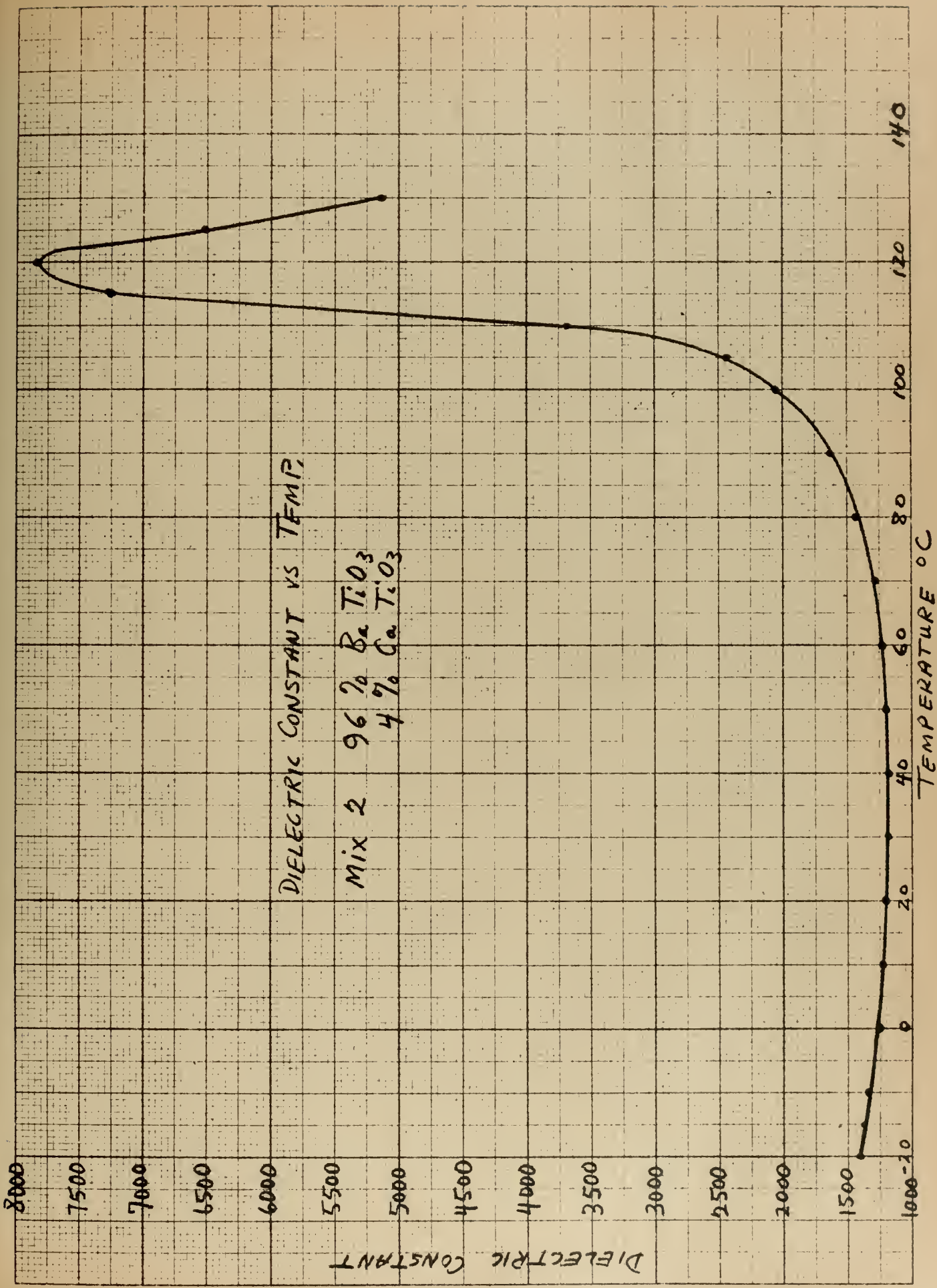


FIGURE 2

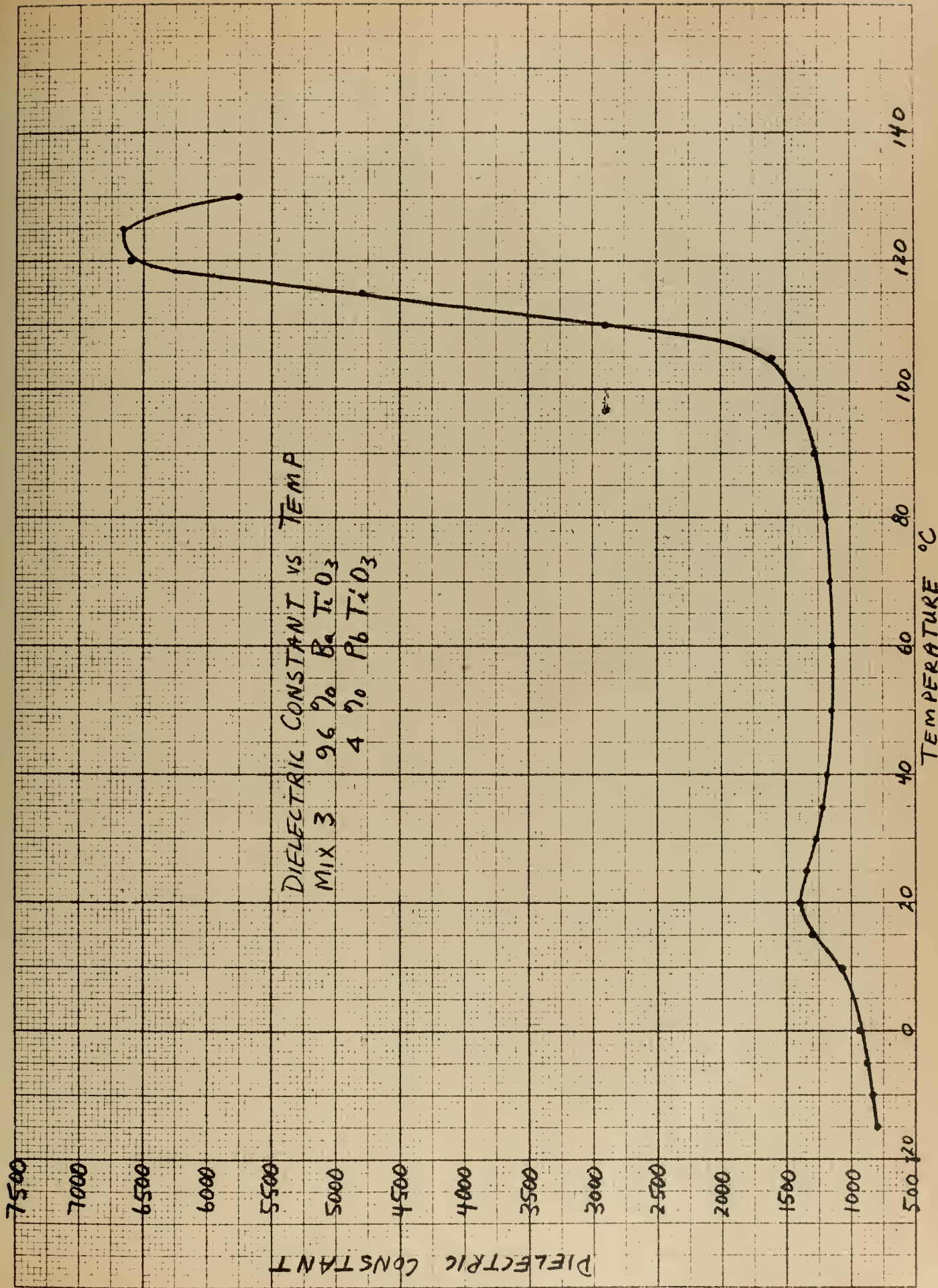


FIGURE 3

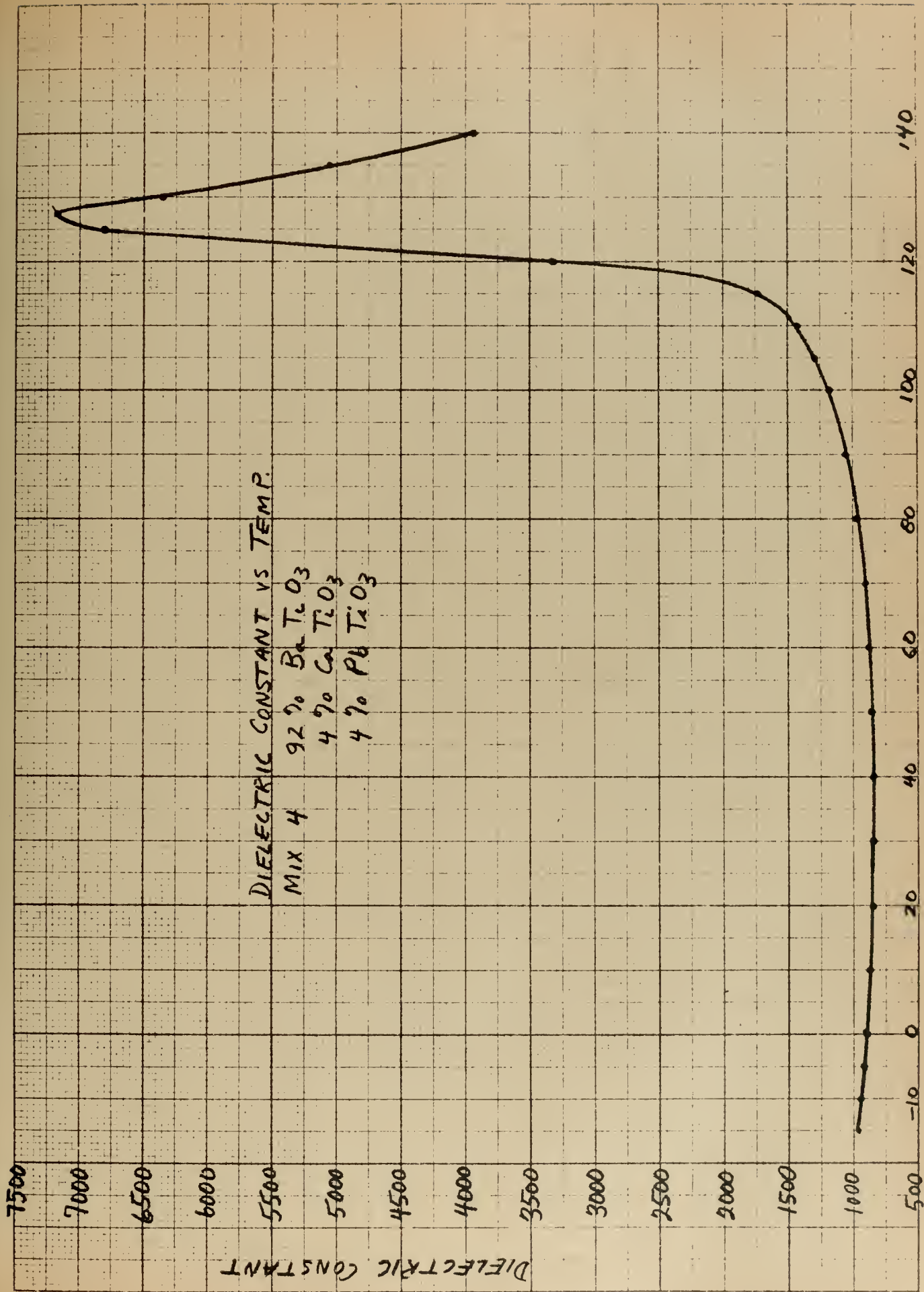
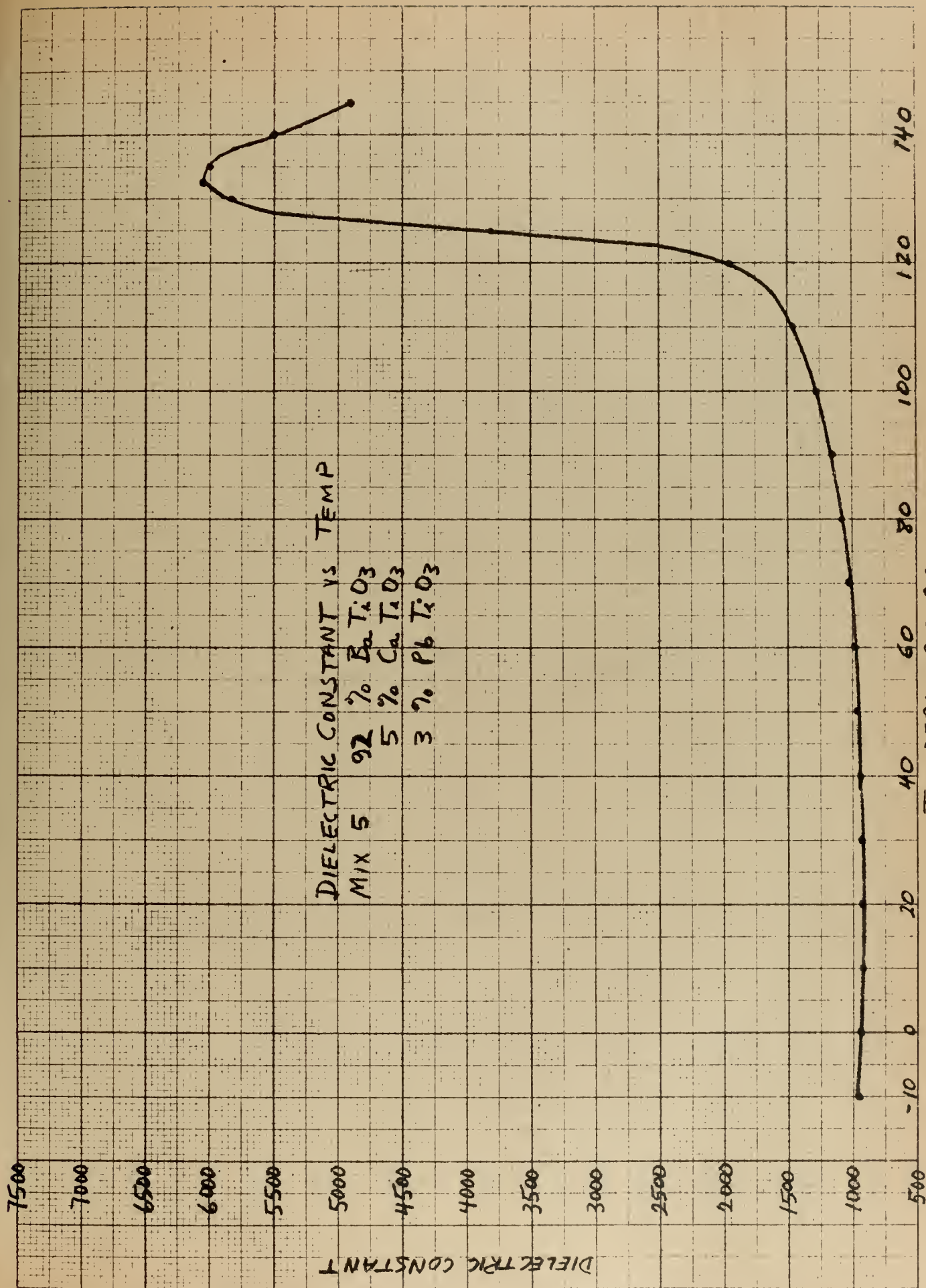


FIGURE 4



TEMPERATURE °C

FIGURE 5

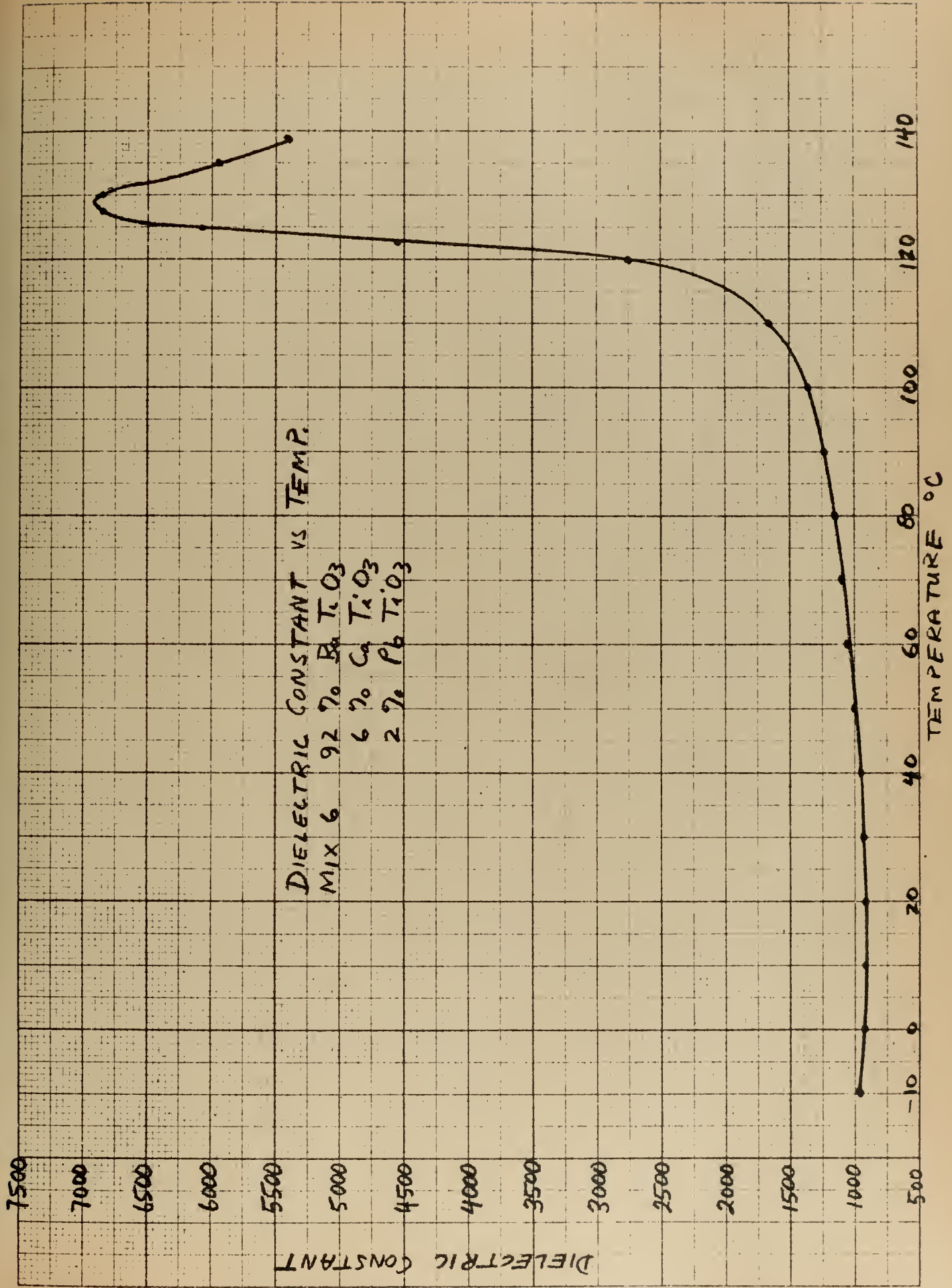


FIGURE 6

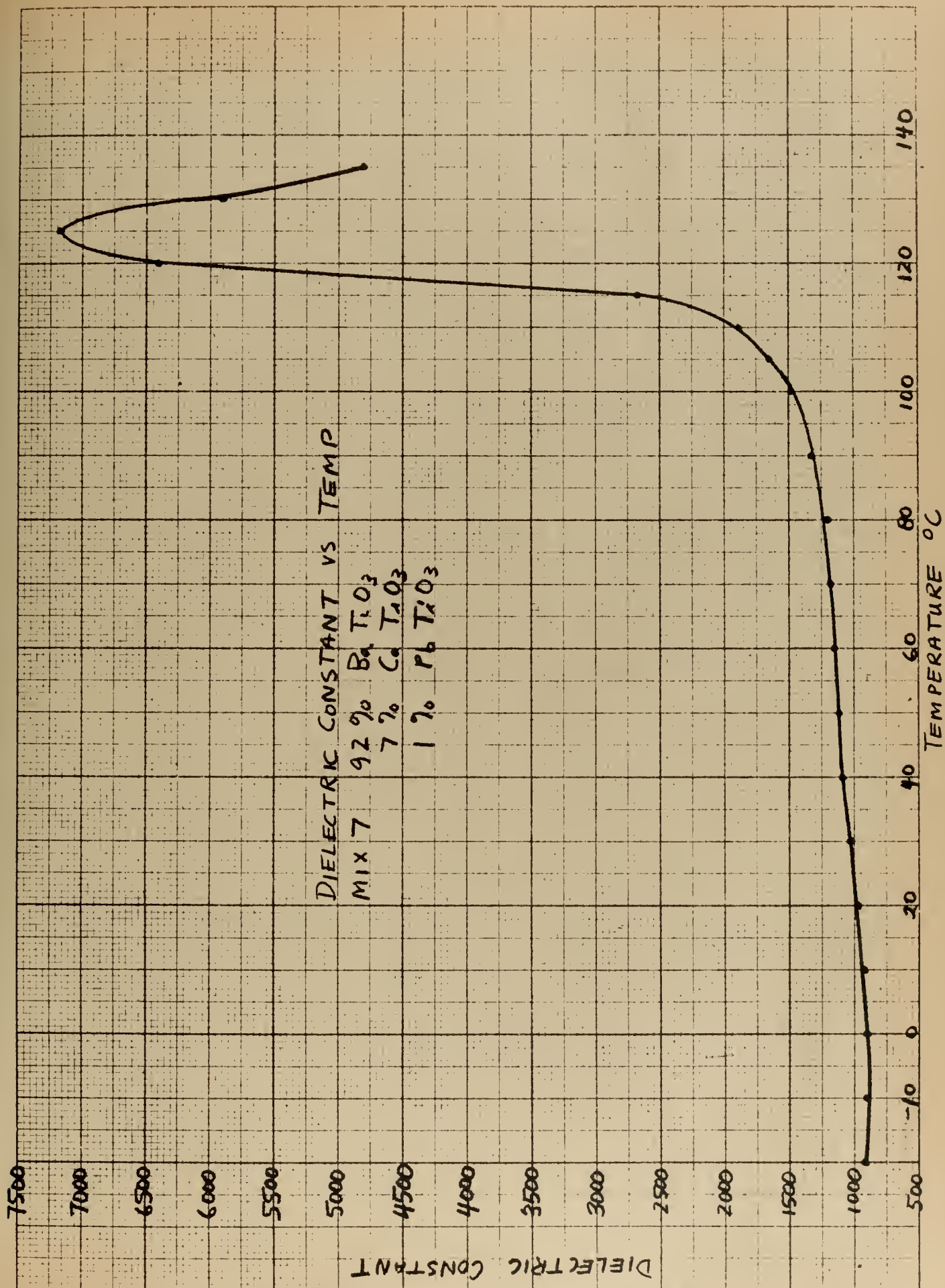


FIGURE 7

temperature variation of crystal properties. An example of this latter property is illustrated in Figure 1, a plot of the free dielectric constant versus temperature for a commercially pure unpolarized barium titanate element of the geometrical configuration used throughout the experiments reported herein (see Chapter IV).

2. Cell structure of barium titanate

The wide variations of crystal properties with temperature are a characteristic of a ferroelectric material and are attributed to a change in the crystal structure of barium titanate. A cell (the smallest regular structure existing within the material) exists in the form of a six-sided parallelepiped, the eight corners being occupied by barium atoms, the six faces by oxygen atoms, and the center by a titanium atom (Figure (8)).

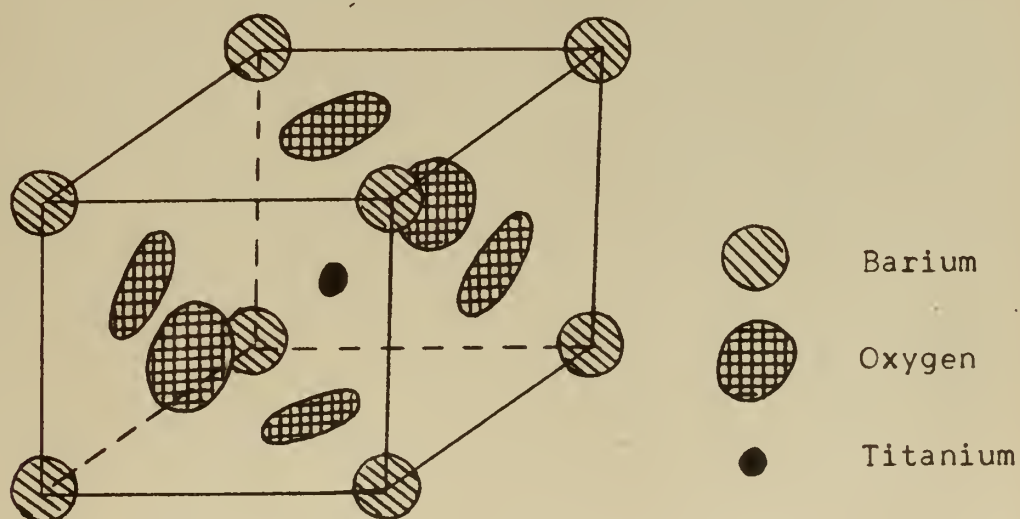


Figure 8

The titanium atom shares a covalent bond with one of the oxygen atoms. Above $120^{\circ}\text{C}.$, the so-called Curie point (a terminology adopted from ferromagnetic theory), there is sufficient thermal energy so that the titanium atom is equally likely to share this covalent bond with any of the six oxygen atoms. There is no net transgression of the titanium from the center of the cell structure and the statistical average of charge center displacement within any domain is zero. The cell thus exists as a cubic structure and there is no polarization or dipole moment formed. Below $120^{\circ}\text{C}.$, the titanium spends all its time in a covalent bond with one of the oxygens. The cell becomes ferroelectric in this direction and exhibits a slight expansion along this axis becoming tetragonal in shape. This condition exists as the temperature is lowered to the second transition point at $20^{\circ}\text{C}.$, at which time the titanium atom shares its time equally in covalent bonds with oxygen atoms along two directions⁽¹⁷⁾ or takes an equilibrium position halfway between two oxygens⁽⁸⁾; the cell becomes ferroelectric along two axes and orthorhombic in shape. At a still lower temperature of approximately $-80^{\circ}\text{C}.$ (not shown in Figure 1), the cell finally becomes ferroelectric along all three axes, trigonal in shape, and it maintains this condition down to absolute zero.

3. Permanent polarization

Although individual cells of barium titanate may thus become spontaneously polarized over a definite temperature

range due to the ferroelectric effect, these cells and the domains which they compose are, in general, randomly oriented within a body of the material so that the body will exhibit no net polarization unless some means is found to encourage the cells to become ferroelectric along the same direction. This can be accomplished by applying a high d-c field to the body. This field induces the titanium to select an oxygen in the general direction of the field so that a component of the polarization will exist in the direction of the applied field. Upon removal of the field the polarization will reduce somewhat, but a remanent polarization approaching 90-95% of saturable polarization will remain⁽²⁾. It was this remanent polarization that led to the discovery of the piezoelectric effect in barium titanate. More refined techniques requiring less polarizing field strengths consist of heating the ceramic element above the Curie point, applying d-c fields up to 20 kilovolts per centimeter, and then cooling under the applied field⁽¹⁷⁾.

4. Hysteresis in ferroelectrics

The wide variation of dielectric constant with temperature has been shown in Figure 1. In addition, the dielectric constant for unpolarized elements varies with applied d-c bias and a-c field strength. The hysteresis loop of electric polarization vs. electric field strength curves indicates that the dielectric constant is a non-linear function of the field strength, and consequently cannot be accurately measured with

a conventional capacitance bridge.

For a linear homogenous dielectric,

$$P = \eta E$$

$$D = E + 4\pi P = E + 4\pi\eta E = (1 + 4\pi\eta) E$$

$$D = KE$$

$$\text{where } K = 1 + 4\pi\eta$$

P = polarization

E = electric field strength

η = electric susceptibility

D = electric displacement

For a ferroelectric material, the total electric polarization

$$P = P_e + P_d$$

where $P_e = AE$

$$P_d = f(E)$$

where P_e = normal electronic and atomic polarization (found in all dielectrics)

P_d = polarization due to dipoles caused by titanium motion

A = constant

$f(E)$ = function of E

Thus $P = P_e + P_d = AE + f(E)$

$$= E[A + f(E)]$$

$$P = Eg(E)$$

$$D = E + 4\pi P = E + 4\pi Eg(E)$$

$$D = [1 + 4\pi g(E)] E$$

$$D = EG(E)$$

$$K = G(E)$$

$$\eta = g(E)$$

The susceptibility and permittivity are both functions of the applied field. Both the displacement-field and polarization-field curves appear as hysteresis loops and it is then possible to define the permittivity in a number of ways (Figure 9).

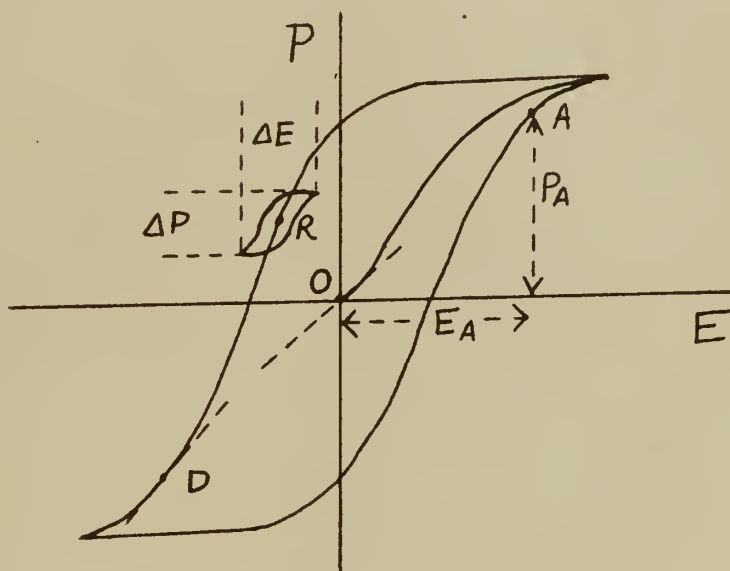


Figure 9

- K_a , the normal permittivity at some point A, $= 1 + 4\pi \frac{P_A}{E_A}$
 K_d , the differential permittivity at some point D, $= 1 + 4\pi \left(\frac{dP}{dE} \right)_D$
 K_o , the initial permittivity at point O, $= 1 + 4\pi \left(\frac{dP}{dE} \right)_{E=0}$
 K_r , the reversible permittivity at some point R for
 a small a-c field $= 1 + 4\pi \left(\frac{\Delta P}{\Delta E} \right)_R$

Hysteresis loops can be closely approximated and observed on a cathode ray oscilloscope by using the bridge circuit of Figure 10⁽⁵⁾, where the vertical deflection is approximately proportional to the charge on the element under test and the horizontal deflection voltage is proportional to the voltage across the test element.

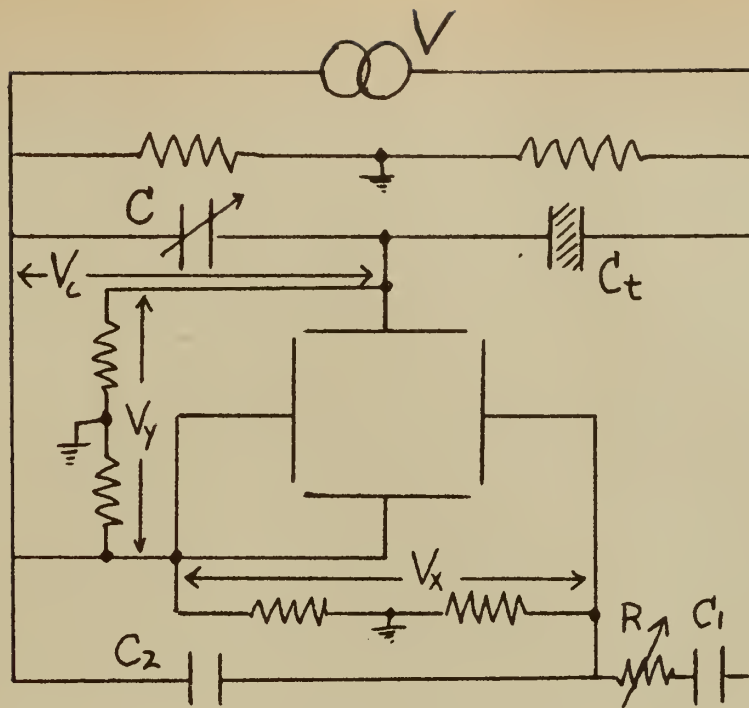


Figure 10

If the resistance across C is sufficiently large, then $Q_c \sim Q_t$ where Q_c is the charge of capacitor C and Q_t is the charge of the test element C_t

$$Q_c = CV_c \sim Q_t$$

$$P_t = \frac{Q_t}{A} \sim \frac{CV_c}{A} = \frac{C}{A} \cdot V_y = \frac{C}{A} s_y \cdot y \quad (2-1)$$

$$V_t = V - V_c$$

$$V_x = \frac{XC_2}{XC_1 + XC_2} \cdot V = \frac{C_1}{C_1 + C_2} \cdot V$$

$$V_t = \frac{C_1 + C_2}{C_1} \cdot V_x - V_c = \frac{C_1 + C_2}{C_1} \cdot V_x - V_y$$

$$V_t = r s_x \cdot x - s_y \cdot y$$

$$E_t = \frac{V_t}{t} = \frac{r s_x \cdot x - s_y \cdot y}{t} \quad (2-2)$$

where A = electrode area of test sample
 P_t = polarization of test sample
 x, y = horizontal and vertical deflection, respectively, in centimeters
 s_x, s_y = horizontal and vertical sensitivity in volts per centimeter
 t = thickness of test sample
 r = $\frac{C_1 + C_2}{C_1}$

The use of Formulae 2-1 and 2-2 permits calibrating the observed curves by measurement of the horizontal and vertical deflection, once the voltage sensitivity of the scope and the values of the necessary circuit parameters are known. It then becomes possible to determine the desired values of permittivity. Furthermore, the area under the curve represents the hysteresis losses in the material under test.

5. Additives to barium titanate elements

From the great number of ceramics investigated in recent years, barium titanate has emerged as the one exhibiting those characteristics most desirable for electromechanical transduction use although, in many instances, the addition of small percentages of additives of titanates or stannates of other elements has improved certain of its properties for special purposes. Considerable research has been done on the effect of these additives upon the dielectric constant of unpolarized ceramics^(19,20,21). In general, it has been found that by spreading the Curie point and the second transition point at 20°C.,



or by simply lowering the latter point, the dielectric constant in the temperature range between these two transitions may be made constant over a wide range of temperatures, or may be made to exhibit constant positive or negative coefficients of temperature over a limited range thereby finding wide application as a temperature compensating capacitor in electronic circuits. While these additives do lower the dielectric constant to some extent, it still remains high compared to other commonly used dielectrics.

For transduction purposes, both lead and calcium titanate additives have proven beneficial. Both lower the second transition point thereby giving a transducer greater temperature stability in this temperature range (Figures 2 - 7). In addition, lead titanate will raise the Curie point somewhat, lower the coefficient of mechanical coupling, render the transducer less susceptible to being depolarized by a high driving field⁽¹⁷⁾, and apparently increase the internal dissipation (Chapter IV). Calcium, on the other hand, appears to decrease the internal dissipation.

6. Comparison of common piezoelectric materials

Ceramic transducer elements compare favorably in some respects and suffer disadvantages in other respects when compared to those piezoelectric crystals that have found extensive use in recent years. The most common of those other elements are quartz, Rochelle Salt (RS), and ammonium dihydrogen phosphate (ADP). Table I shows a comparison of some of the



important electromechanical constants of these crystals⁽¹³⁾.

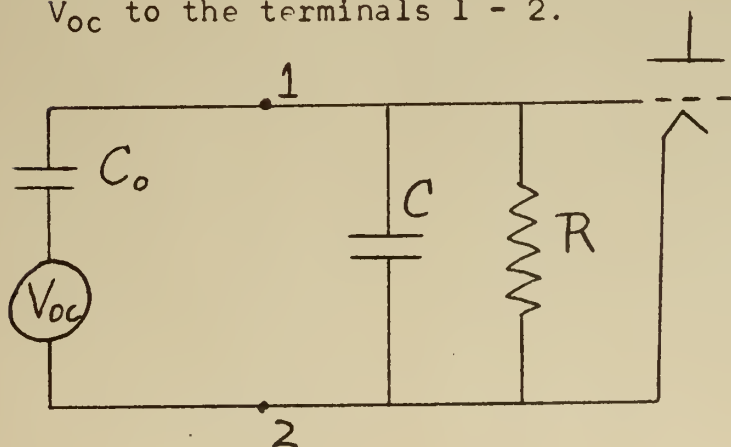
The d coefficients represent the ratio of strain to applied field or short circuit current per applied force. The g coefficients represent the ratio of open circuit voltage to applied force or strain to applied charge. The third column lists the elastic modulus, Y, and the fourth column the ratio of voltage out to applied strain, which is simply the product Yg since $Y = T/S$ where T = stress and S = strain.

TABLE I

	1	2	3	4	5
	d	g	Y	Yg	Coeff. of coupling
CRYSTAL	10^{-12}m/V	$\frac{\text{V-m}}{\text{Newton}}$	10^9Newtons/M^2	10^9V/m	$k^2 = dgY$
Rochelle Salt					
X-cut lateral	165	.093	19.3	2.9	.29
Y-cut lateral	27	.33	10.7	3.6	.093
ADP					
Lateral	24	.177	19.3	3.4	.084
Quartz					
Lateral and parallel	2.3	.058	80	4.6	.011
Barium Titanate (Brush Ceramic A)					
Parallel	190	.0125	110	1.38	.26
Lateral	78	.0052	110	.57	.045

It can be readily seen from the first column that barium titanate (with the driving field applied parallel to the axis of polarization) far exceeds any other in motor action (motion for field in) and is approached only by X-cut Rochelle Salt in

this respect. These two also exceed all others in coefficient of electromechanical coupling (Column 5), the significance of which is explained in a later chapter. Column 2 indicates that, on the other hand, barium titanate as a voltage generator for an applied stress is considerably less sensitive than any of the other materials shown, although the high value of elastic modulus causes a relatively better showing in voltage produced for an applied strain (motion). This apparent shortcoming of barium titanate as a voltage generator (that is, as a receiving hydrophone) is somewhat compensated for by the high dielectric constant of the ceramic which considerably reduces the effects of associated circuit loading due to cable capacities and input admittance to electronic amplifiers. This permits a greater portion of the generated open circuit voltage to be recovered from the ceramic hydrophone than from other crystals with their much lower dielectric constants. For a hydrophone operating below resonance in the region of flat response, Figure 11 represents a simple equivalent circuit⁽¹¹⁾. If C_0 is large, the transducer then represents a low internal impedance voltage source and will deliver a large fraction of V_{oc} to the terminals 1 - 2.



C_0 = electric capacity of transducer

C, R due to cable and input to tube

V_{oc} = open circuit voltage of transducer

Figure 11

The very attractive advantages of the ceramics are their relatively low cost, availability, and the fact that they can be pressed, slip cast or extruded into a variety of desired shapes such as discs, cylinders, spheres, bowls (sections of spheres), and bars. Additionally, they can have their electric axes "put in" in any direction that electrodes can be conveniently placed, rather than having to accept the natural coordinate systems of other crystals, permitting their use in a wide number of applications. Figure 12 illustrates some of the more common modes of vibration and polarizing techniques. The arrows on the left hand model of each type illustrate the manner of applying the original d-c polarization. For the disc of Figure 12a, a field applied parallel to the polarization produces a strain both parallel and at right angles (transverse), to the applied field. The latter strain is less than the former so a net change in volume results. This configuration may thus be used in parallel (or thickness) mode, transverse (or radial) mode or in the volume expander mode. The "squirting cylinder" mode of Figure 12b has proven popular in underwater sonics; here the outer surface and one end may be covered with a pressure release material so that radiation occurs from the inner surface only. This causes a pressure wave to be transmitted from the open end either directly into the surrounding medium in a free-flooded transducer, or through a sound transparent window into the sea. Here transverse coupling is used, the radial driving field producing a circumfer-

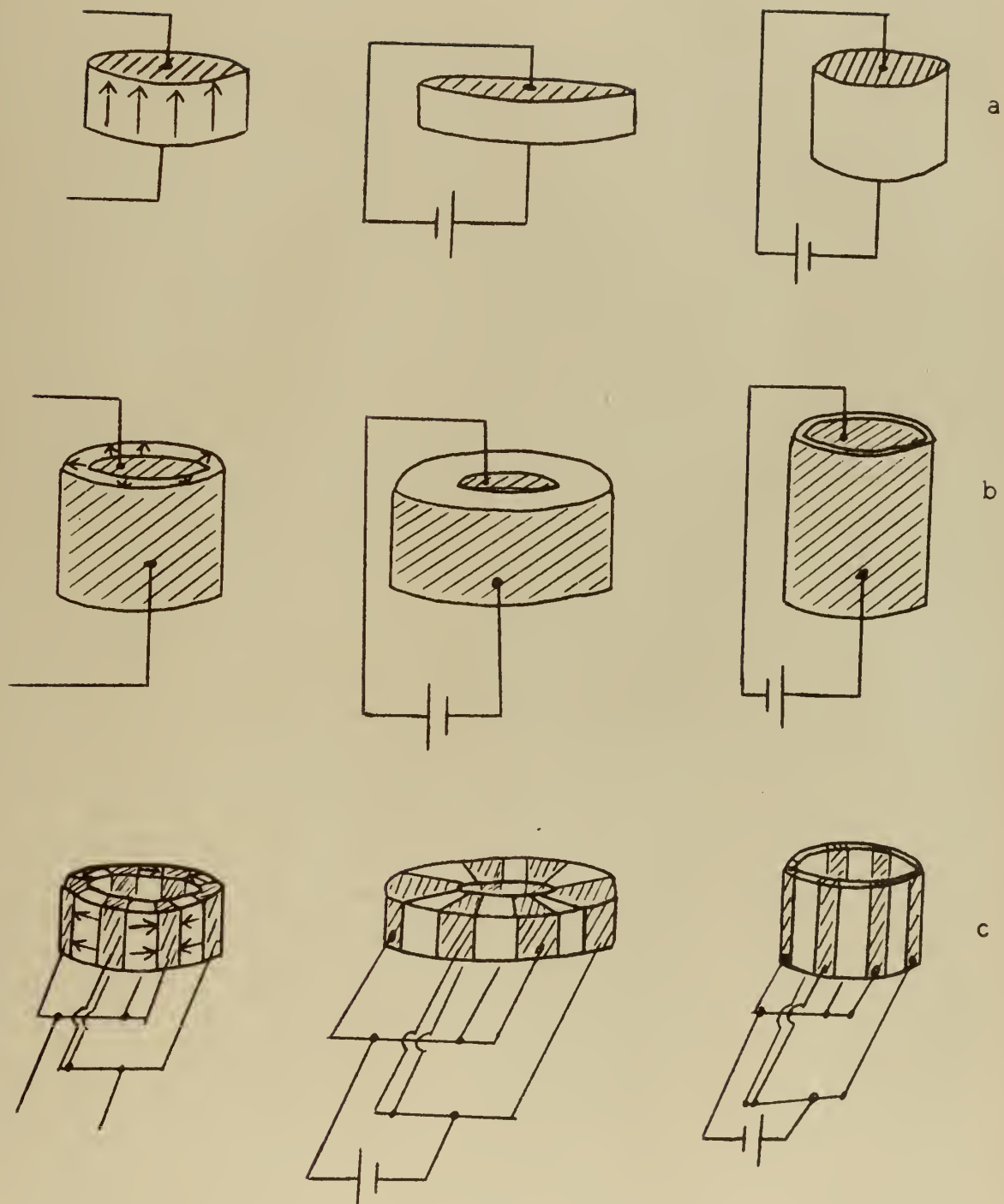


Figure 12

ential strain naturally resulting in a radial expansion and contraction. Figure 12c represents a means of driving the circumferential mode directly, polarization and driving field being applied circumferentially.

The fact that these ceramics can be so easily handled and shaped is linked to a major disadvantage. The ultimate electromechanical properties depend a great deal upon the exact techniques used in mixing, forming, firing and polarizing in addition to the amounts of trace impurities (to be distinguished from deliberately added additives) that may exist in the raw barium titanate powder. This is so much in evidence that elements of the exact same dimensions, mixed and treated from the same materials in the same manner, may exhibit relatively large dispersion in the electromechanical activity and resonant frequency. Variations from lot to lot of the raw titanate may be even greater. The reasons for much of this anomalous behavior are not known today.

CHAPTER III

ANALYSIS OF AN ELECTROMECHANICAL NETWORK

1. Transduction coefficients

An electromechanical system may in general be represented by the four terminal network shown in Figure 13 where T_{em} and T_{me} are transduction coefficients, T_{em} relating the effect of the mechanical mesh upon the electrical mesh and T_{me} the reverse effect. These coefficients may be complex and are either symmetric ($T_{em} = T_{me}$) or unsymmetric ($T_{em} = -T_{me}$). A well-known example of unsymmetric coefficients

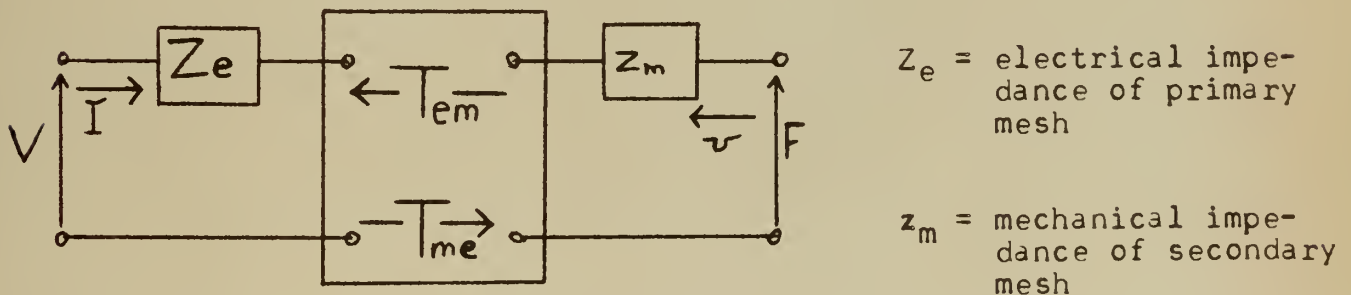


Figure 13

occurs in the electromechanical coupling characteristic of motor and generator action. In the latter, a moving wire has induced in it an emf, $V = B\ell v$, where B is the magnetic flux density, ℓ the length of wire, and v the velocity of the wire in the magnetic field. Conversely, in motor action the force

on a moving wire, $F = B\ell I$, where I is the current in the wire. In neither of the above formulae is any sense of direction given. This is generally determined by applying Fleming's right and left hand rules for generator and motor respectively, or by writing the equations in vector notation, i.e., $\vec{V} = \ell(\vec{v} \times \vec{B})$ and $\vec{F} = \ell(\vec{I} \times \vec{B})$. However, if the directions of V and I and of F and v are taken to coincide in a given application, then $V = -B\ell v$ and $F = B\ell I$ may be written from which the unsymmetrical transduction coefficients $B\ell$ and $-B\ell$ are recognized at once.

The mesh equations may be written from Figure 13, as

$$V = Z_e I + T_{em} v \quad 3 - 1$$

$$F = T_{me} I + z_m v \quad 3 - 2$$

from which

$$T_{em} = (V/v)I = 0 \quad (\text{primary open})$$

$$T_{me} = (F/I)v = 0 \quad (\text{secondary clamped})$$

2. Motional impedance

$$\text{From Equation 3 - 1, } Z_{in} = V/I = Z_e + T_{em} v/I \quad 3 - 3$$

$$\text{and from Equation 3 - 2, } F/v = T_{me} I/v + z_m \quad 3 - 4$$

If F/v is replaced by $-Z_L$, the mechanical load impedance across the secondary, then

$$-Z_L = T_{me} I/v + z_m$$

$$v/I = \frac{-T_{me}}{z_m + Z_L} \quad 3 - 5$$

Substituting 3 - 5 in 3 - 3

$$Z_{in} = Z_e + \frac{-T_{em} T_{me}}{z_m + Z_L} \quad 3 - 6$$

where Z_{in} is the electrical driving point impedance of the

electromechanical system and is seen to consist of two components, Z_e , the purely electrical impedance of the electrical primary, and the term $-\frac{T_{me} T_{em}}{z_m + Z_L}$ which is the electrical impedance seen at the input due to mechanical motion in the secondary. For this reason, the latter term is called the motional impedance of the system.

$$Z_{mot} = - \frac{T_{me} T_{em}}{z_m + Z_L} \quad 3 - 7$$

$$Z_{in} = Z_e + Z_{mot}$$

A study of the motional impedance of a transducer can provide a good deal of information regarding its operation. Replacing $z_m + Z_L$ by Z_M , the total secondary mechanical impedance including both that due to the vibrating element and any loading effects due to the medium into which it is radiating, and by setting $T_{me} = T_{em} = T$ (symmetrical transduction coefficients) which is valid for a piezoelectric type element

$$/ \quad Z_{mot} = - \frac{T^2}{Z_M} = - T^2 Y_M \quad 3 - 8$$

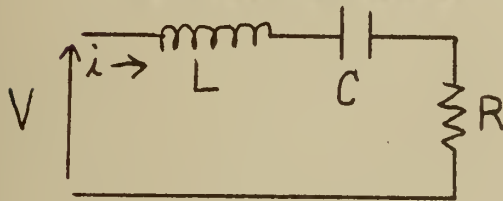
The significance of the transduction coefficient is readily seen. It is an operator, having in general both magnitude and phase, and a units converter which, when operating upon a mechanical admittance, changes it into an electrical impedance.

If now the differential equations are written for the motion of a mechanical system having mass, compliance and damping, they are seen to be completely analogous to the equations for the current in an RLC electrical circuit, the configuration

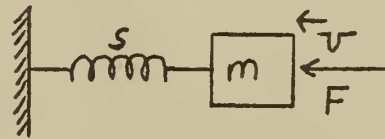
of the circuit depending upon the drive conditions selected.

A simple example is cited here.

Electrical Circuit



Mechanical Circuit



x = displacement
m = mass
s = stiffness

$$V = L \frac{di}{dt} + \frac{1}{C} \int i dt + Ri$$

$$F = m \frac{d^2x}{dt^2} + R_m \frac{dx}{dt} + sx$$

$$\frac{dV}{dt} = L \frac{d^2i}{dt^2} + R \frac{di}{dt} + \frac{1}{C}i$$

$$F = m \frac{dv}{dt} + R_m v + s \int v dt$$

$$\omega_o = \sqrt{\frac{1}{LC}}$$

$$\frac{dF}{dt} = m \frac{d^2v}{dt^2} + R_m \frac{dv}{dt} + sv$$

$$\omega_o = \sqrt{\frac{1}{m/s}} = \sqrt{\frac{1}{m C_m}}$$

The following analogies are evident:

Voltage, V, analogous to Force, F

Current, i, analogous to Velocity, v

Inductance, L, analogous to Mass, m

Capacity, C, analogous to $\frac{1}{\text{stiffness}}$, $\frac{1}{s}$, or mechanical com-

pliance, C_m

Resistance, R, analogous to mechanical resistance, R_m

The validity of the above analogies is easily demonstrated. If the mass is infinite, there can be no motion in the mechanical circuit; if the inductance is infinite (open), no current

flows in the electrical circuit; if the spring has infinite stiffness (zero compliance), no motion occurs; if the electrical capacity is zero, no current can flow (open circuit).

With electromechanical vibrating elements, we deal with distributed constants rather than the lumped constants illustrated in the above mechanical circuit. There are, furthermore, many different modes of vibration possible and many harmonics of each mode. Nevertheless, for any particular mode in the frequency region around a resonance, the crystal may be represented by an equivalent lumped circuit containing a mass, compliance and resistance which may be expressed in terms of the density, dimensions, dielectric constant, compliance and piezoelectric coefficients. By virtue of the analogy previously drawn, the mechanical impedance of the equivalent lumped circuit including loading effects may then be written

$$Z_M = R_M + j \left(\omega M - \frac{1}{\omega C_m} \right)$$

where R_M , M and C_m represent the equivalent lumped mechanical resistance, mass and compliance respectively.

$$Z_M = R_M + jX_M$$

$$Y_M = \frac{1}{Z_M} = G_M - jB_M = \frac{R_M}{R_M^2 + X_M^2} - j \frac{X_M}{R_M^2 + X_M^2}$$

letting $\theta = \tan^{-1} \frac{B_M}{G_M} = \tan^{-1} \frac{X_M}{R_M}$

$$\cos \theta = \frac{R_M}{\sqrt{R_M^2 + X_M^2}} = \frac{R_M}{|Z_M|} = R_M |Y_M|$$

then $|Y_M| = \frac{1}{R_M} \cos \theta$ 3 - 9

Since R_M is a constant in the region of the resonance selected, and θ varies from approximately -90° to $+90^\circ$ as the frequency is varied through resonance, the mechanical admittance describes a circle if plotted in the polar plane (Figure 14a).

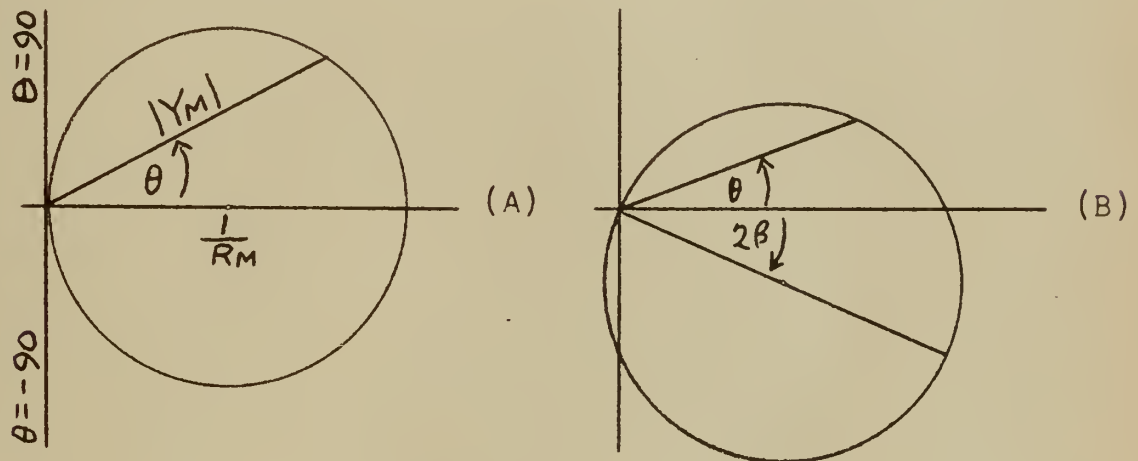


Figure 14

Substituting 3 - 9 in 3 - 8

$$Z_{\text{mot}} = -T^2 Y_M = T^2 |Y_M| e^{j\theta} = \left[\frac{-T^2}{R_M} \cos \theta \right] e^{j\theta}$$

$$Z_{\text{mot}} = \left[\frac{-T^2}{R_M} \cos \theta \right] \cos \theta + j \left[\frac{-T^2}{R_M} \cos \theta \right] \sin \theta$$

$$Z_{\text{mot}} = R_{\text{mot}} + j X_{\text{mot}}$$

The variation of the motional impedance depends upon the nature of $-T^2$. In the case of piezoelectric transduction, T inherently contains a time quadrature factor which will eliminate the troublesome negative sign carried through to this point. Thus, if we let $T = jA$, then $-T^2 = A^2$ where A^2 is the vector force factor defined by Hunt⁽¹²⁾. A will, in the simplest case, be a real constant but may become complex due to hysteresis

losses, eddy currents or dielectric absorption⁽¹²⁾. If A is complex, let

$$A = |A|e^{j\beta} \quad \text{where} \quad \beta = \tan^{-1} \frac{\text{Im}(A)}{\text{Re}(A)}$$

then $A^2 = |A|^2 e^{j2\beta}$ and $Z_{\text{mot}} = |A|^2 Y_M e^{j2\beta}$

The effect of an imaginary component of A is then to rotate the motional impedance circle by an angle 2β , as shown in Figure 14b, where A has been assumed to contain a negative reactance component.

3. Efficiency

The diameter of the motional impedance circle is seen to be inversely proportional to the total mechanical resistance which is the sum of the external loading resistance and the internal damping resistance. Since these two resistances represent the only sources of mechanical energy dissipation, a measure of the mechanical efficiency of the element can be obtained if the relative values of these two resistances are known. If the element is placed in air, the loading impedance is so slight that the diameter, D_A , of the motional impedance circle in air is then inversely proportional to the mechanical damping resistance, R_m . Similarly, if the element is loaded by water, the diameter D_W is inversely proportional to the sum of R_m and the loading resistance, R_L .

Then,

$$D_A = \frac{I^2}{R_m} \quad 3 - 10$$

$$D_W = \frac{I^2}{R_m} = \frac{I^2}{R_m + R_L} \quad 3 - 11$$

from which

$$\frac{R_L}{R_m + R_L} = \frac{D_A - D_W}{D_A}$$

3 - 12

the "mechanical utilization" factor of the transducer.

The total efficiency may be defined as the ratio of acoustic power out to electrical power in.

$$P_{out} = |v|^2 R_L = \left| \frac{F}{Z_M} \right|^2 R_L$$

$$P_{in} = |I|^2 R_{in}$$

$$\eta = \frac{P_{out}}{P_{in}} = \frac{|v|^2 R_L}{|I|^2 R_{in}} = \left| \frac{v}{I} \right|^2 \frac{R_L}{R_{in}}$$

From 3 - 5,

$$\frac{v}{I} = \frac{T_{me}}{Z_m + Z_L} = \frac{T}{Z_M}$$

at resonance

$$\frac{v}{I} = \frac{T}{R_M}$$

$$\left| \frac{v}{I} \right|^2 = \frac{|T|^2}{R_M^2}$$

$$\eta_{res} = \frac{|T|^2 R_L}{R_M^2 R_{in}} = \frac{D_W R_L}{R_M R_{in}} = \frac{D_W R_L}{R_{in} R_M}$$

From 3 - 12,

$$\frac{R_L}{R_M} = \frac{D_A - D_W}{D_A}$$

Then

$$\eta_{res} = \frac{D_W}{R_{in}} \frac{D_A - D_W}{D_A}$$

3 - 13

4. Electromechanical coupling coefficient

A generalized equivalent electrical circuit for a piezo-electric transducer around resonance is shown in Figure 15.

C_0 represents the pure electrical capacitance of the crystal due to its geometry, that of a dielectric between two conducting plates. Losses have been neglected. L , C and R are here electrical quantities dependent upon the mechanical and piezoelectric properties of the crystal and also upon the transduction coefficient.

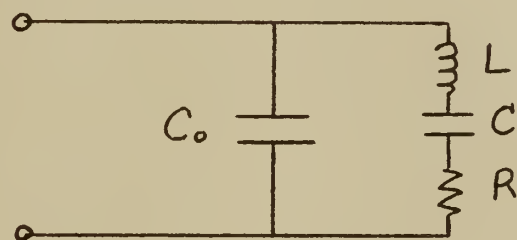


Figure 15

Such a circuit will exhibit two resonance frequencies, a series resonance, f_r , of the series arm and a parallel resonance, f_a , when the series arm becomes inductive and resonates with C_0 . The separation of these two frequencies is determined by the relative values of C and C_0 , and since these capacities represent the amounts of energy that may be stored in the circuit mechanically (due to crystal distortion) and electrically, respectively, the separation of f_r and f_a represent a measure of the mechanical activity or electro-mechanical coupling factor. Mason⁽¹⁷⁾ has shown that, for the ceramic disc in radial vibration (the configuration used in these experiments), the electromechanical coupling coefficient is

$$k = \sqrt{2.51 \frac{f_a - f_r}{f_r}}$$

This is very simply approximated by observing the current into a transducer as the frequency is varied under constant input voltage conditions. The current maximum and minimum then indicate frequencies of impedance minimum and maximum from which k may be determined. The coefficient of electromechanical coupling is intimately related to the Q of the transducer and bandwidth considerations⁽²³⁾. A high k is desirable for broad bandwidth response.

INPUT IMPEDANCE CIRCLE IN AIR

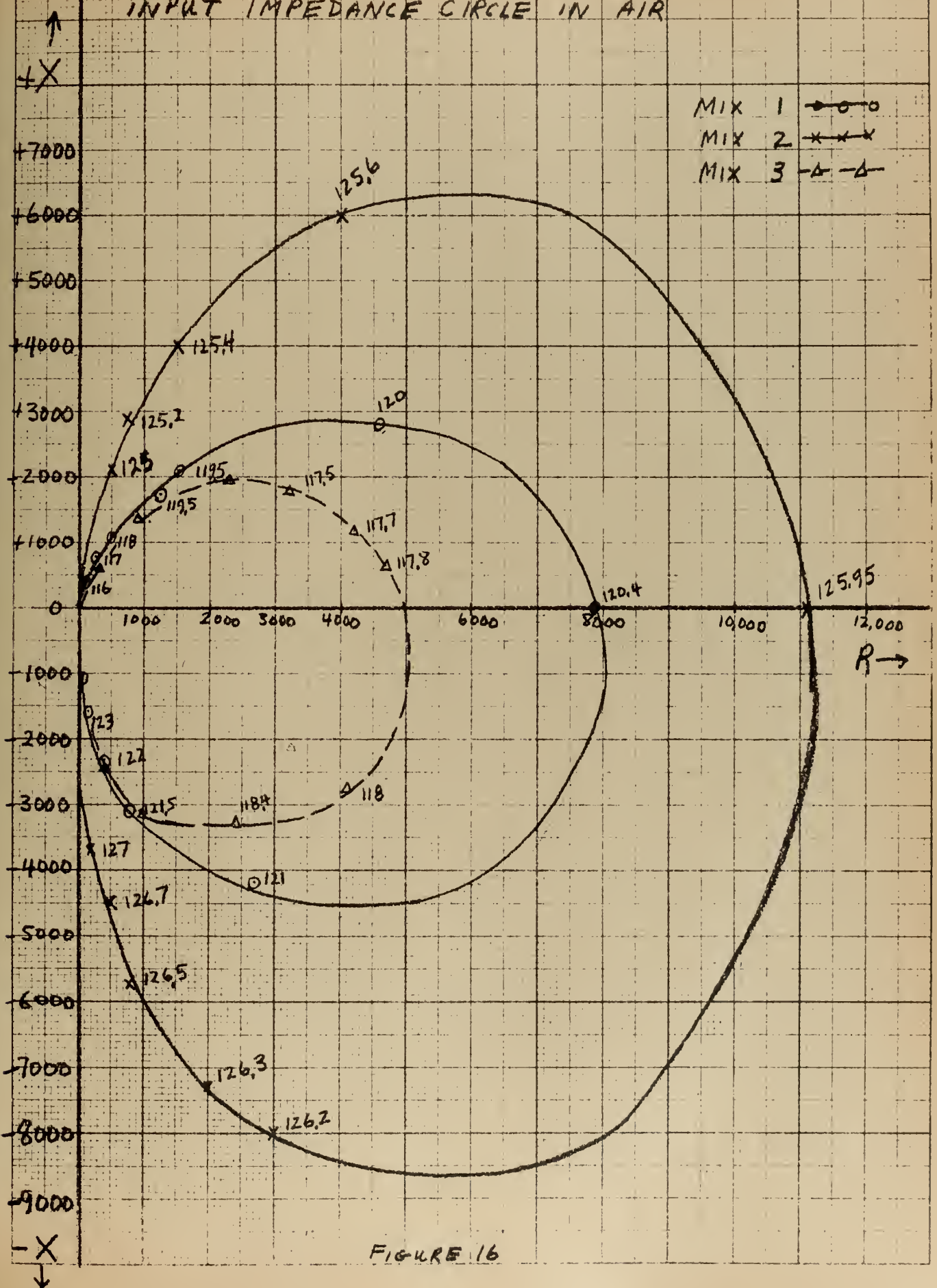


FIGURE 16

INPUT IMPEDANCE CIRCLE IN AIR

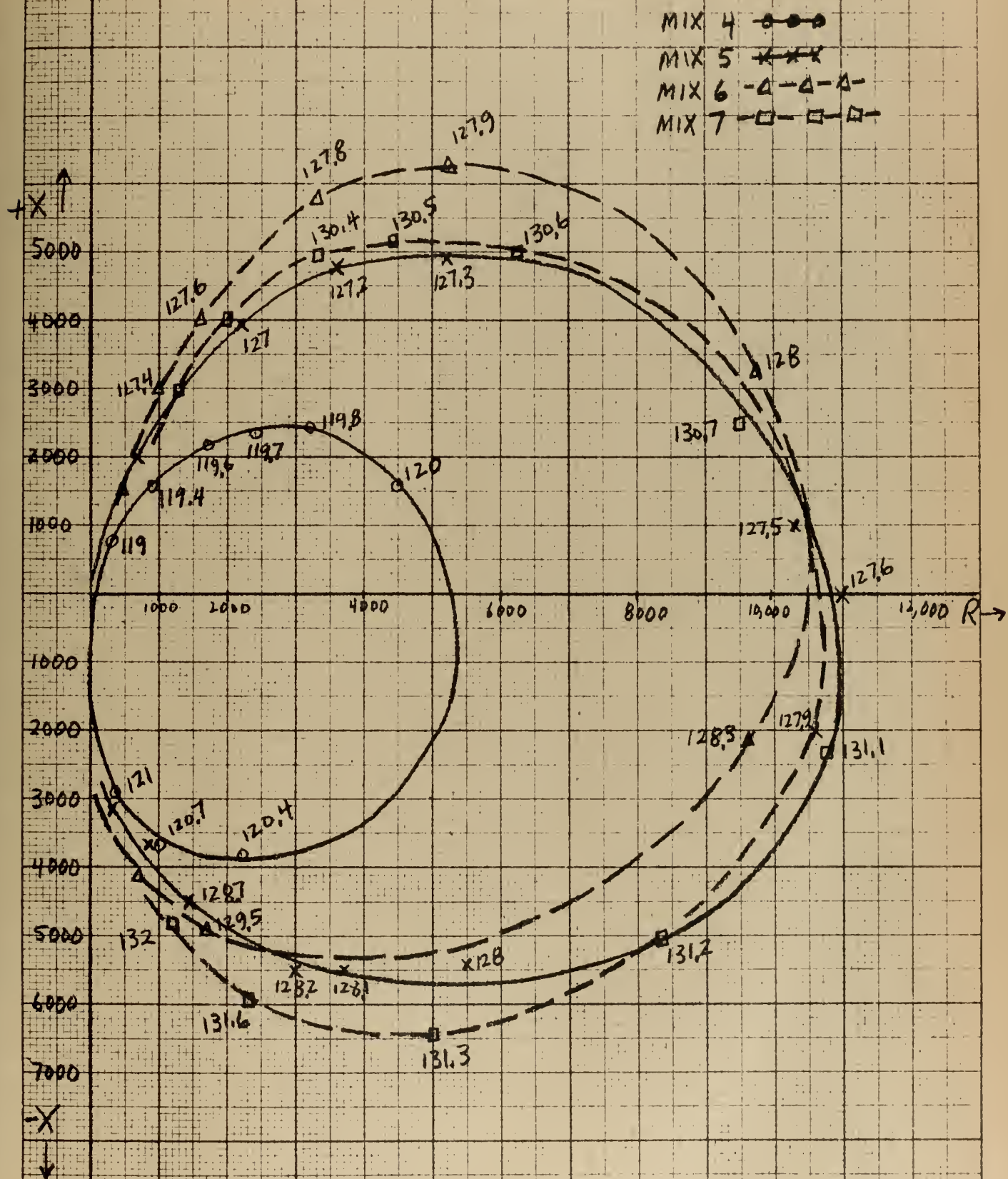


FIGURE 17

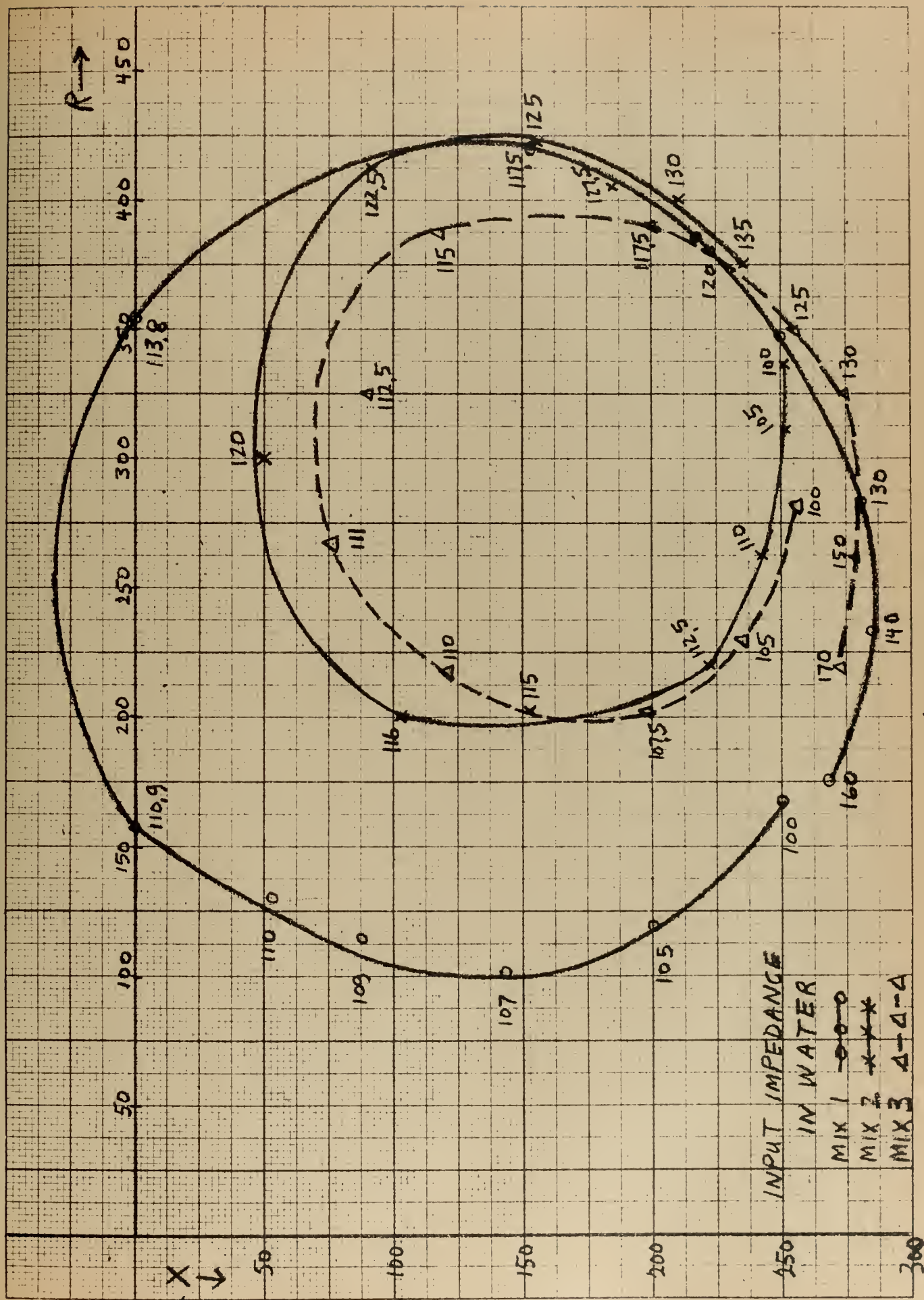


FIGURE 18

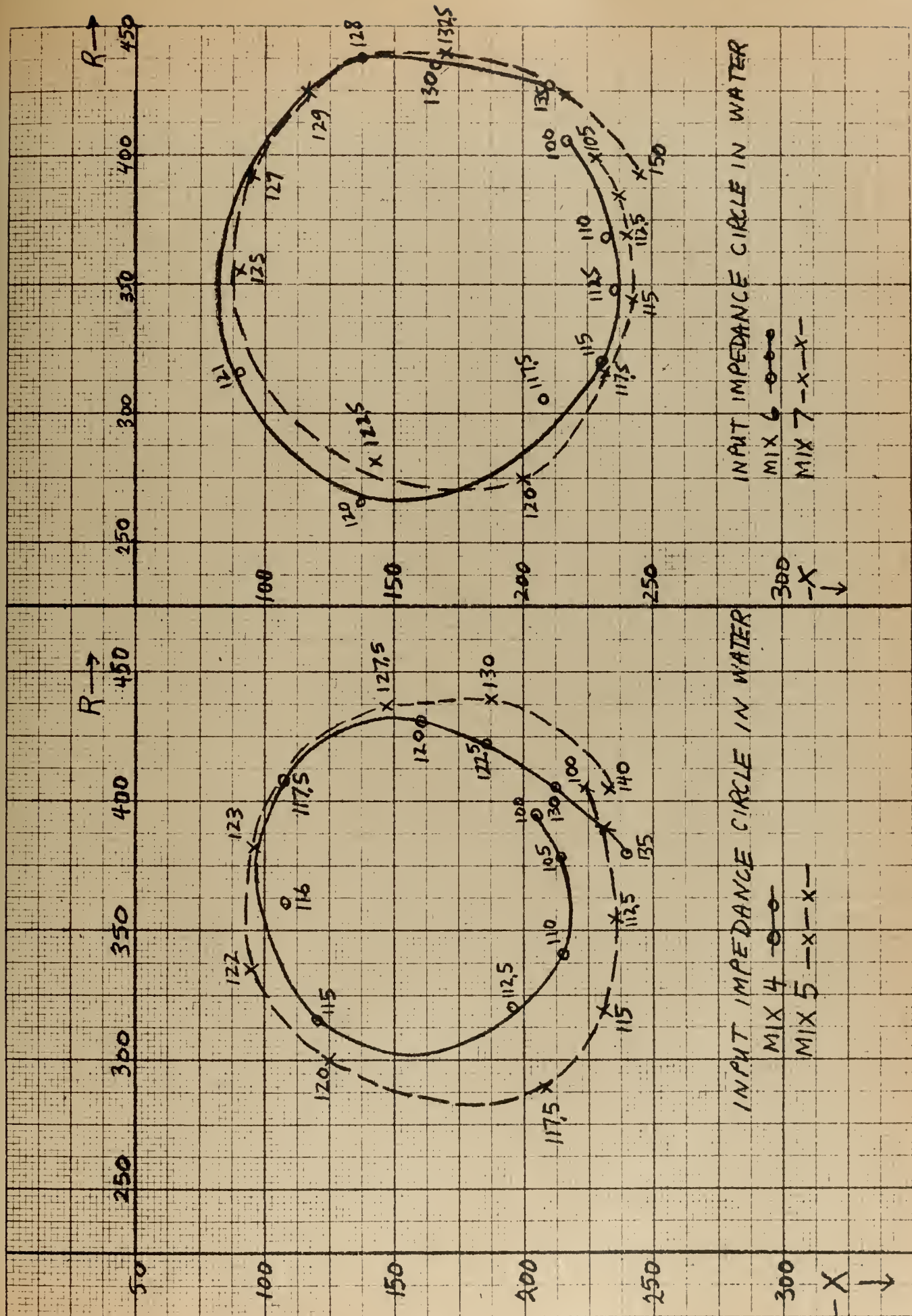


FIGURE 19

A TYPICAL FIRING CYCLE

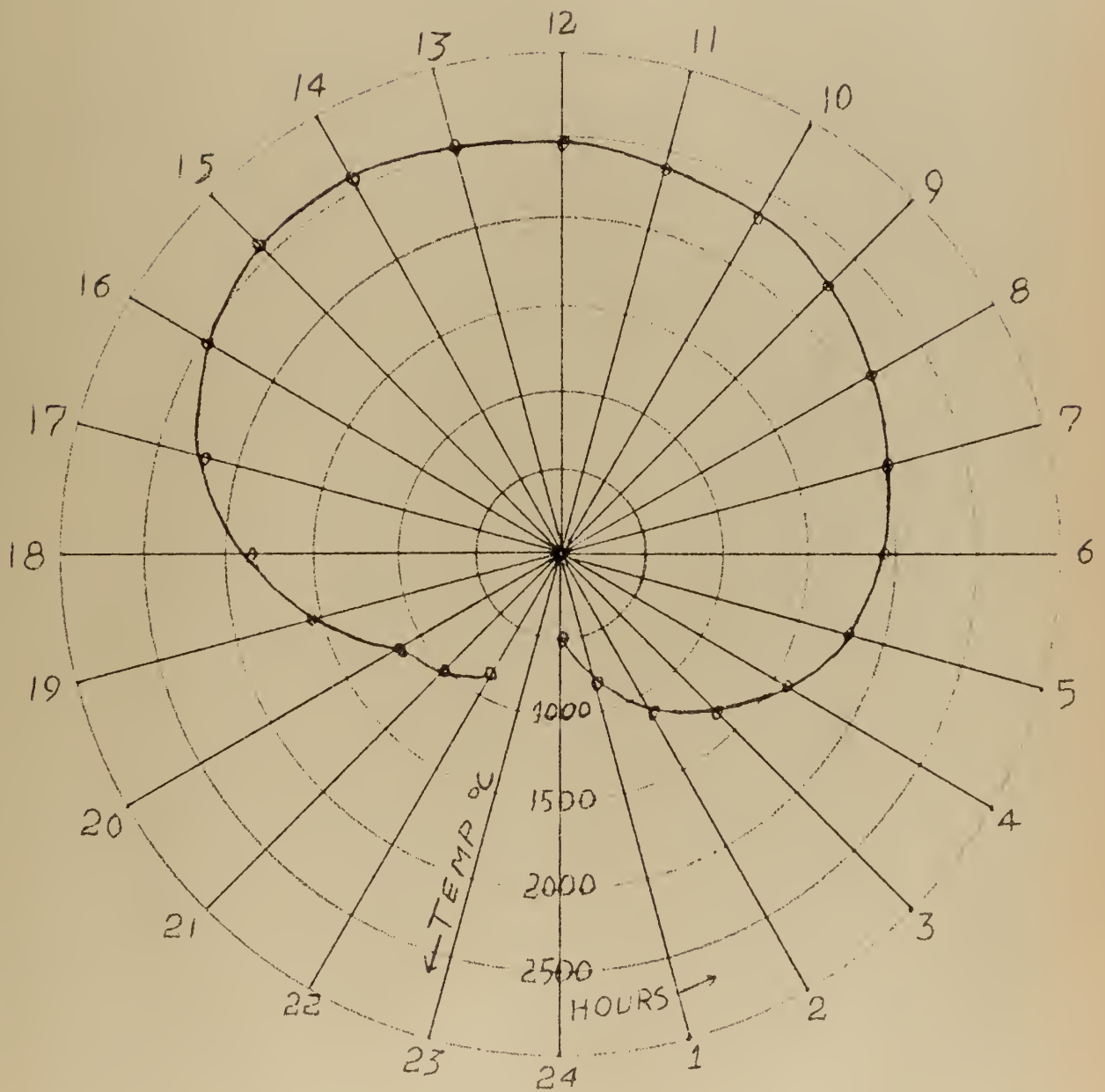


FIGURE 20

CHAPTER IV
EXPERIMENTAL WORK

1. Preparation of the test samples

It has already been mentioned that calcium and lead titanate additives to barium titanate elements have appeared to offer the most promising resulting effects upon the ultimate electromechanical properties of ceramic transducers. For this reason, seven different mixtures in varying percentages of these substances were prepared with two basic ideas in mind. First, that the total percentage of barium titanate should be large, and second, that the percentage of lead titanate should be no greater than the calcium titanate due to the extra internal dissipation associated with lead titanate additives. The percentages by weight for each of the mixtures are indicated in Table II.

TABLE II

MIX	% BaTiO_3	% CaTiO_3	% PbTiO_3
1	100	0	0
2	96	4	0
3	96	0	4
4	92	4	4
5	92	5	3
6	92	6	2
7	92	7	1

The form of the test elements was chosen as a disc for simplicity of construction. Using this geometry, the elements could be pressed into the desired form rather than requiring either slip casting or extrusion processes generally applicable to other shapes of ceramic elements.

The three titanates are obtained commercially in a fine powder form. A bonding agent of three per cent liquid wax (Socony Vacuum Foamrex S) and seven per cent distilled water was thoroughly mixed with the powder after which the desired samples were pressed at 7500 pounds per square inch pressure. The dimensions of these "raw" discs were approximately .15 inches thick and somewhat less than one inch in diameter, the ultimate dimensions of the prepared samples being less and varying slightly from lot to lot due to slightly different shrinkage in firing. A typical firing cycle is reproduced in Figure 20. After firing and cleaning, electrodes were applied to the faces of the discs by painting on a solution of Du Pont silver paste No. 4822 mixed with toluol to a brushing consistency and then fired on at 1470°C.

Polarizing presented somewhat of a problem. In experimenting with various polarizing field strengths, it soon became apparent that those mixes containing a large percentage of lead titanate were prone to break down at lower field strengths than other samples. Thus the problem appeared to be which was the fairer way to judge the relative properties of the various mixes; to subject them all to the same low polarizing field strength

or to polarize each at the highest field strength that it would withstand. The former approach was chosen for two reasons. First, the time element **precluded** a thorough investigation into maximum polarizing field strength and, second, the loss of elements which would be encountered due to breakdown in such an investigation would reduce the number of elements available for test. A modest figure of 14.6 kilovolts per inch was selected.

2. Philosophy of measurements

In Chapter II it was stated that it is not unusual for the electromechanical properties of identical samples made from the same mix to vary from sample to sample. For this reason, six elements from each mix were measured for density, unpolarized dielectric constant at room temperature, electromechanical coupling coefficient and "activity", the latter quantity as represented by the number of decibels between current into the polarized element at minimum and maximum impedance as measured with a conventional **impedometer** circuit. It was then possible to choose one element from each mix which could be considered as representative of that mix and apply further tests to these "average" samples.

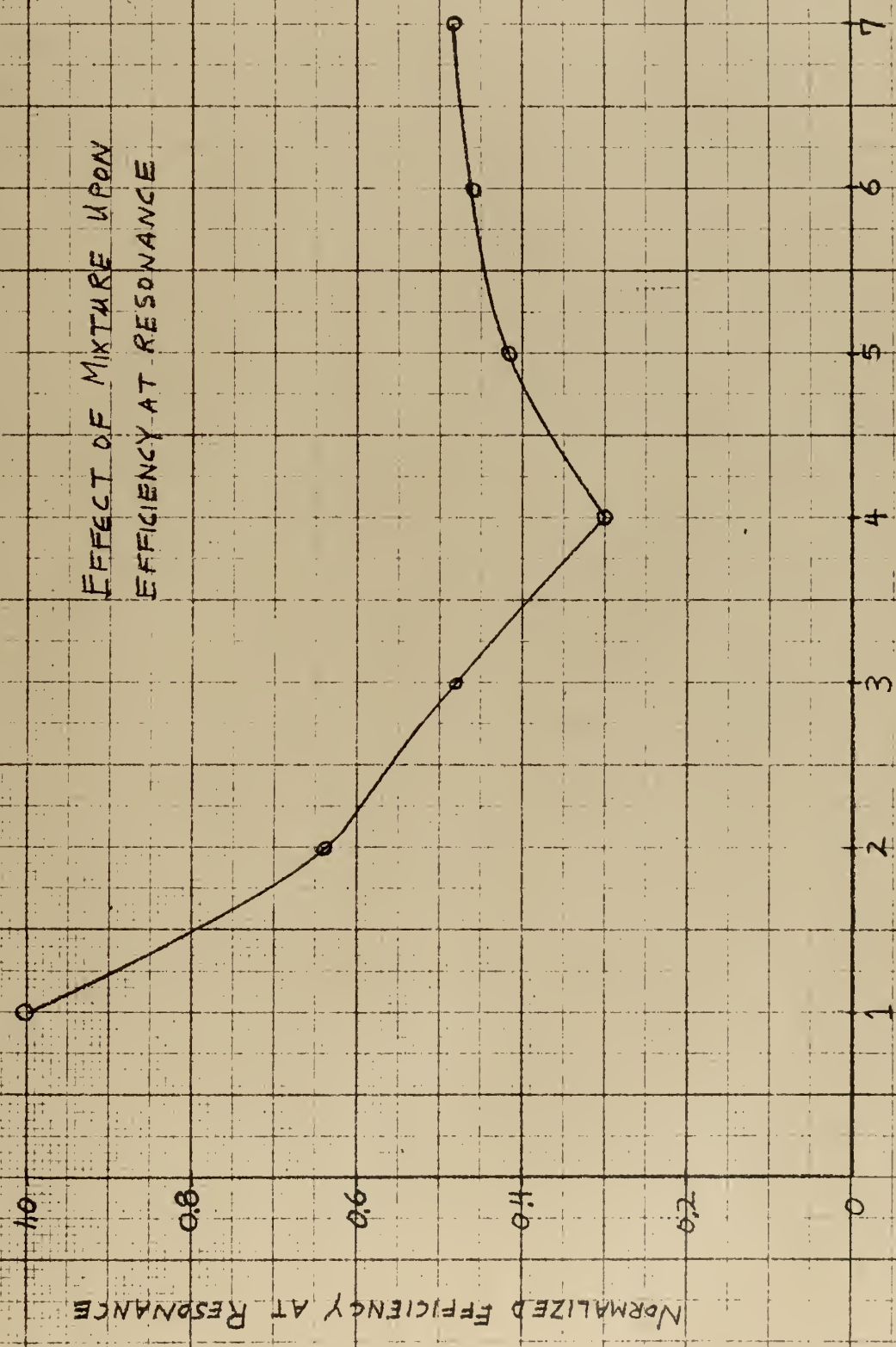
3. Total impedance diagrams and efficiency at resonance

The total impedance circles for seven sample elements are reproduced in Figures 16 through 19. The Q of the elements is sufficiently high in air so that the diameter of the motional impedance circle can be closely approximated by taking the diameter of the total impedance circle. The diameter of the

motional impedance circle in water must be derived from Figures 18 and 19 by subtracting out the electrical impedance graphically. By also noting the mechanical resonant frequency from the motional impedance circle, the input resistance at resonance can be determined and the efficiency at resonance computed from Formula 3 - 13. The results of these computations are illustrated Figure 21 where all efficiencies have been normalized to that of Mix 1 since we are interested only in relative figures. The actual values of efficiency are somewhat meaningless. This is so since no realistic loading of the test elements was attempted or considered necessary. The discs were completely immersed in water with all surfaces radiating, a situation impractical on any real transducer. Consequently, the radiation resistance, R_L , the "mechanical utilization" factor and the computed efficiency at resonance will all be quite high. It is further expected that mass loading will also be present since the circumference of the disc is approximately two wave lengths, and this is evidenced by some reduction in the frequency of mechanical resonance when the disc is placed in water.

A study of Figure 21 indicates several interesting facts. First, that any additive will reduce the efficiency of a plain barium titanate transducer. Second, the lead titanate is much more damaging than is the calcium titanate as a comparison of the relative efficiencies of Mix 2 and 3 indicates. This latter fact is demonstrated quite well when it is observed that in Mix-

EFFECT OF MIXTURE UPON
EFFICIENCY AT RESONANCE



MIX NUMBER

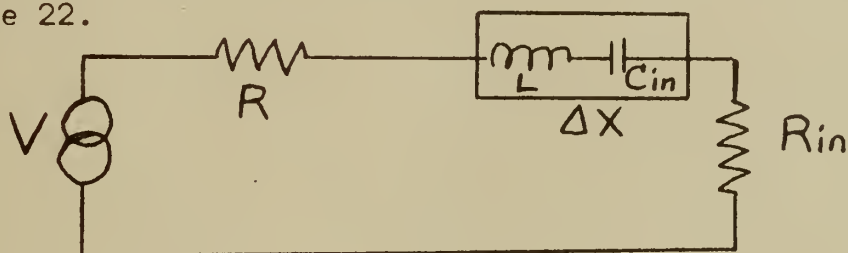
FIGURE 21

es 4 through 7 as the lead is removed and replaced by calcium, the efficiency steadily increases. It can be estimated that approximately twice as much calcium titanate additive can be used than lead titanate for the same reduction in efficiency. The small diameter of the Mix 3 motional impedance circle in air substantiates the conclusion that a high mechanical damping resistance can be attributed to lead titanate additives with a consequent loss of efficiency.

4. Variation of input impedance with temperature

With any ferroelectric material, variation of properties with temperature is a major disadvantage. For that reason, in this section the temperature variation of input impedance of the seven samples is investigated. In an underwater piezoelectric transducer, it is customary to tune out the capacitive reactance when matching the transducer to its driving amplifier by inserting either a series or parallel inductance depending upon whether a low or high resistance input is desirable. Inasmuch as the series input impedance is readily available from the input impedance circles in water, we choose here a series inductance. It is necessary at this point to make several arbitrary decisions before a tuning inductance can be chosen. First, an operating frequency must be selected and this is chosen, for each sample, as the frequency for which the input resistance is maximum, that is, on the right hand extremity of the input impedance circle. Second, since the input impedance can be assumed to be a function of temperature also, the inductance tuning can be totally effective at only one tempera-

ture. Again arbitrarily, this temperature is chosen as 10°C . in all instances. Last, we assume that the driving amplifier has been matched to the transducer for maximum power transfer (that is, the output resistance of the amplifier is equal to the input resistance to the transducer at the frequency and temperature chosen) and that the tuning coil chosen is lossless. The circuit now under consideration then appears as in Figure 22.



$$\Delta X = X_L - X_{in} = 0 \quad \text{at } 10^{\circ}\text{C and chosen frequency}$$

$$R = R_{in} \quad \text{at } 10^{\circ}\text{C and chosen frequency}$$

Figure 22

At the selected frequency and temperature,

$$P'_{out} = |I|^2 R'_{in} = \frac{V^2}{(R + R'_{in})^2} R'_{in} = \frac{V^2}{4R'_{in}} = \frac{V^2}{4R}$$

where the primed values of P_{out} , R_{in} , and I denote those values occurring at the chosen operating point.

At any other temperature,

$$P_{out} = |I|^2 R_{in} = \frac{V^2}{|Z|^2} R_{in} = \frac{V^2}{(R + R_{in})^2 + (\Delta X)^2} R_{in}$$

$$\frac{P_{out}}{P'_{out}} = \frac{V^2 R_{in}}{(R + R_{in})^2 + (\Delta X)^2} \cdot \frac{4R}{V^2} = \frac{4R R_{in}}{(R + R_{in})^2 + (\Delta X)^2}$$

Now, expanding the square term in the denominator and dividing numerator and denominator by R^2

$$\frac{P_{out}}{P'_{out}} = \frac{4 \frac{R_{in}}{R}}{1 + 2 \frac{R_{in}}{R} + \frac{R_{in}^2}{R^2} + \left(\frac{\Delta X}{R}\right)^2}$$

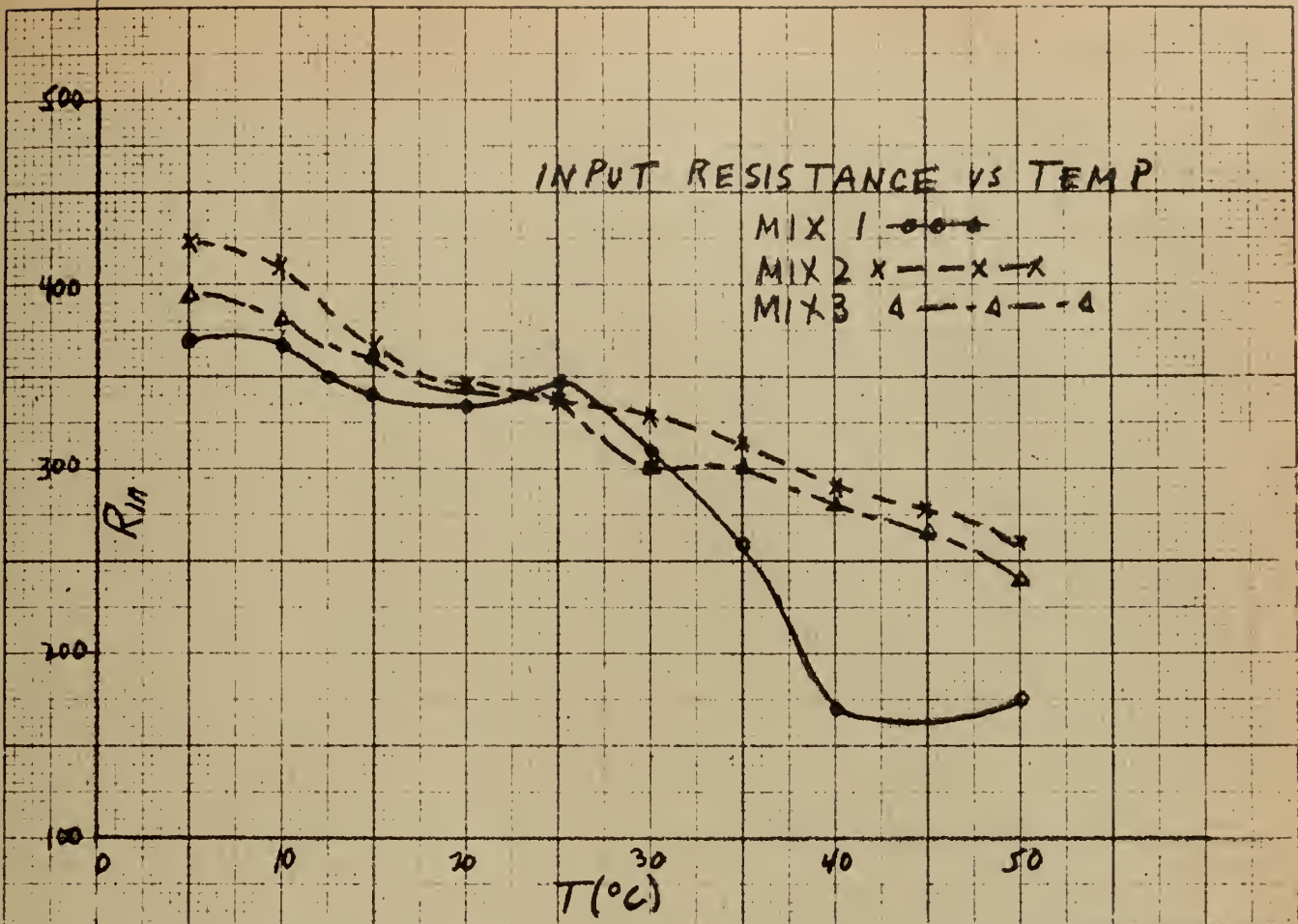
$$\frac{P_{out}}{P'_{out}} = \frac{4r}{1 + 2r + r^2 + x^2}$$

where r and x indicate that the input resistance and net reactance have been normalized to R (or R'_{in}).

Figures 23 and 24 indicate the variation of input resistance and reactance respectively with temperature of the seven different samples. The range of temperatures chosen represents those which might be encountered at sea. The comparatively large fluctuations of the 100% barium titanate mixture are at once evident and this can be attributed to the presence of a transition point in the temperature range. One fact is at once clear and that is that the amount of additive to the barium titanate appears to be the determining factor rather than the proportions of lead and calcium additives. The disappearance of the large fluctuations in those mixes containing percentages of lead and calcium titanate is a result of shifting the transition point down in temperature as was illustrated in the plots of dielectric constant versus temperature in Figures 1 through 7. The importance of these variations of resistances and reactances is in their effect upon the power that can be delivered to the transducer. This is more easily seen by referring to the curves of Figure 25 where the loss in power relative to that delivered under the initially

INPUT RESISTANCE VS TEMP

MIX 1 $\circ-\circ-\circ$
 MIX 2 $x---x---x$
 MIX 3 $\Delta---\Delta---\Delta$



INPUT RESISTANCE VS TEMP

MIX 4 $\circ-\circ-\circ$
 MIX 5 $x---x---$
 MIX 6 $\Delta---\Delta---$
 MIX 7 $\square---\square---$

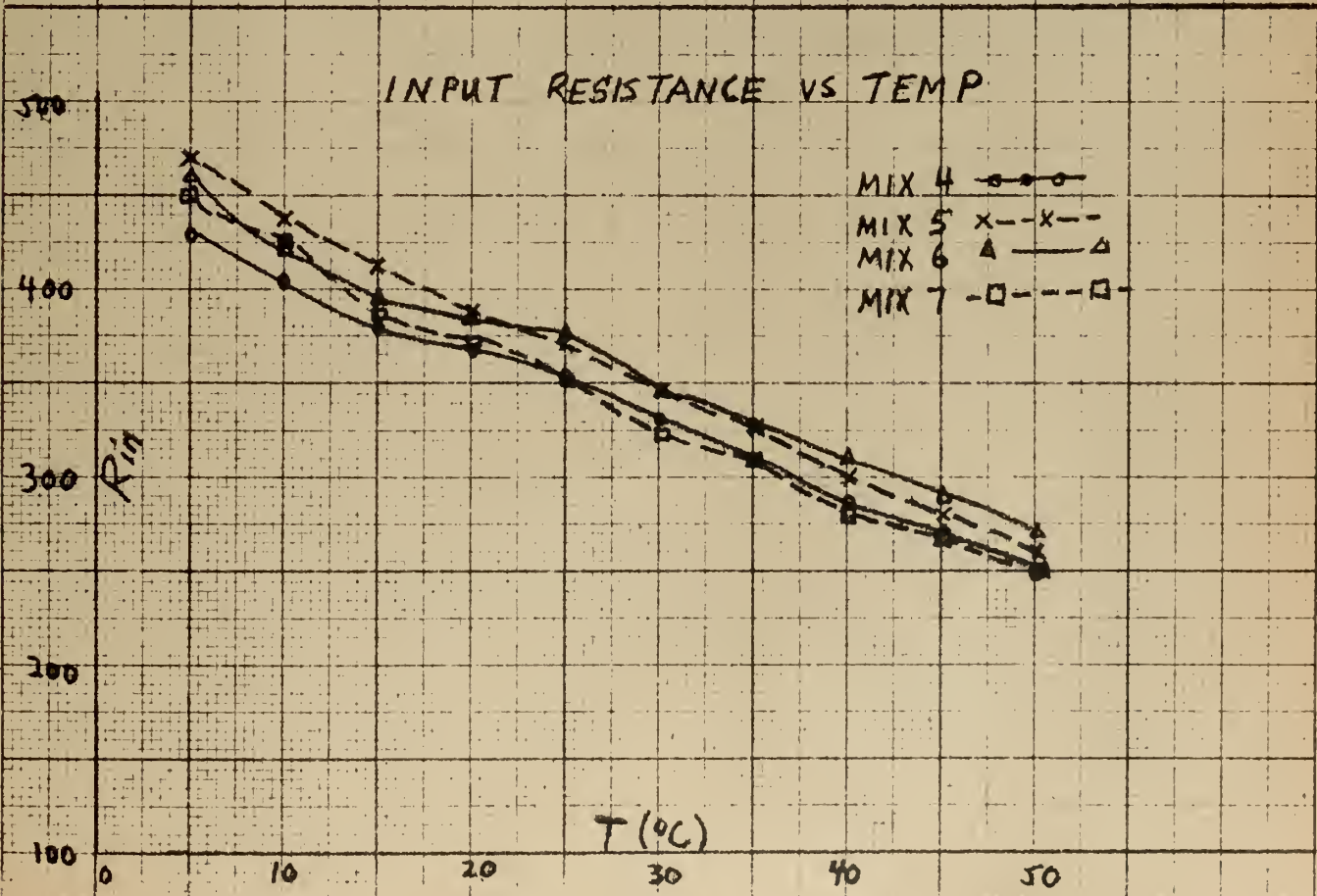


FIGURE 23

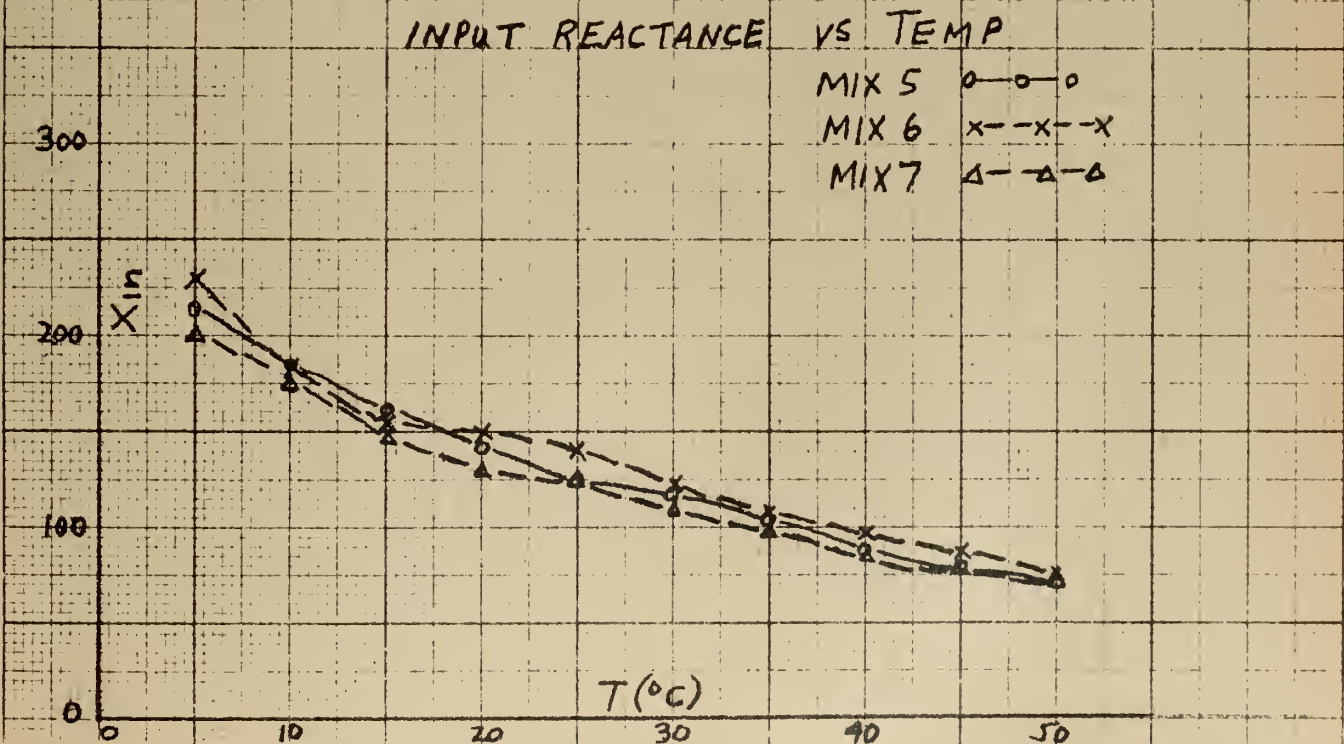
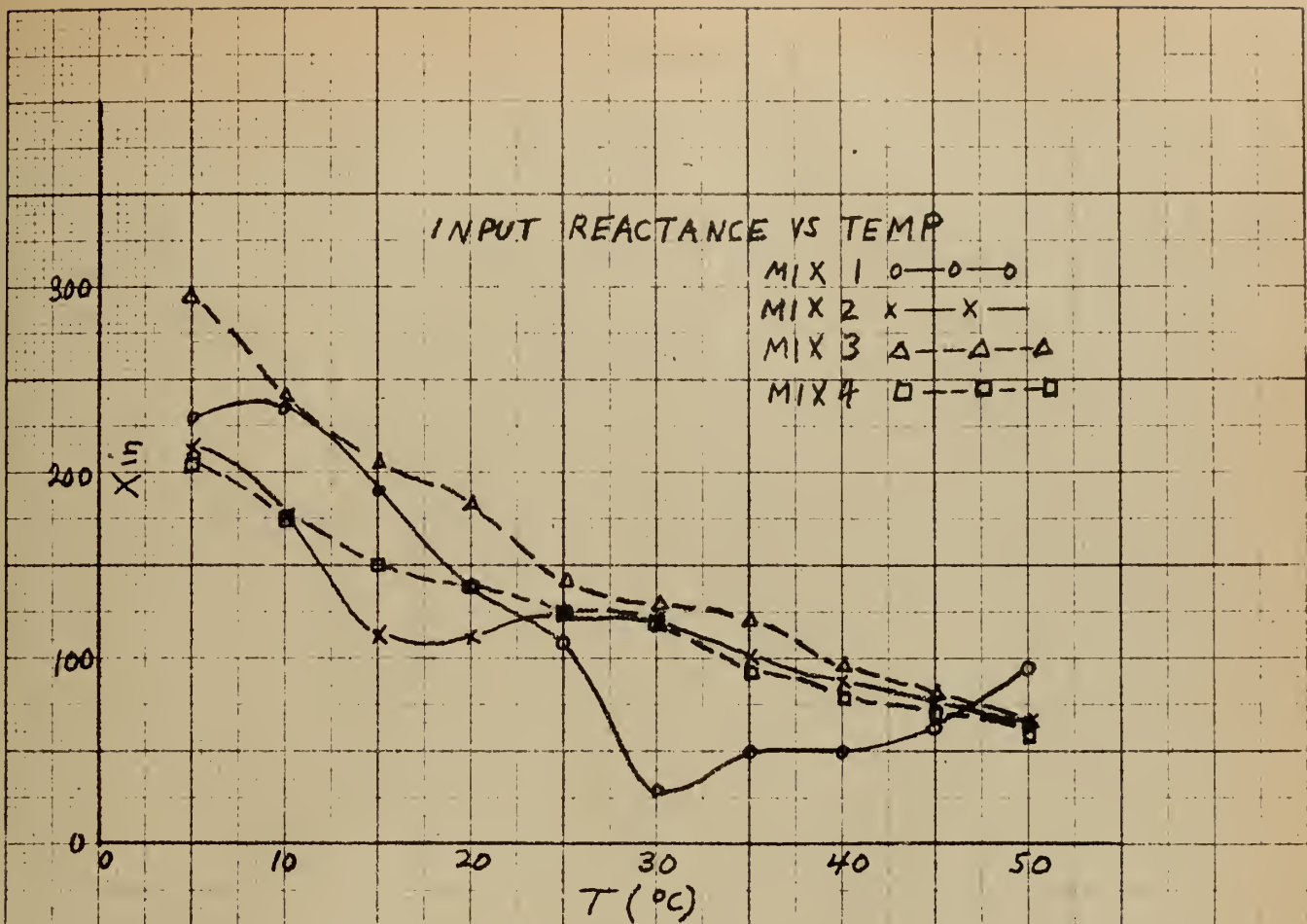


FIGURE 24

assumed conditions is shown. It is here evident that Mixes 4 through 7 all show approximately the same magnitude of variation, and there is little to choose from one to the other. Furthermore, the four per cent calcium (Mix 2) appears to be on a par with these, while the four per cent lead (Mix 3) improves the plain barium titanate but does not show as much effect as the others.

5. Electromechanical coupling coefficient

The electromechanical coupling coefficient was measured in air by the method outlined in Section 4 of Chapter II for all of the samples of each mix. The figures presented here represent an average for the six test elements of each mix tested and do not differ by more than several tenths from the coupling coefficient of the particular sample chosen from each mix for the impedance and power tests already described. Here again the total percentage of additive appears to be the determining factor, there being a marked decrease in coupling coefficient in going to the four per cent (Mixes 2 and 3) and the eight per cent (Mixes 4 - 7) additive mixtures. (See Figure 26). There is no significant difference in the coupling coefficients of Mix 2 and 3 indicating no preference in this respect for lead or calcium. There is a marked increase in going from Mix 4 to 5, but this increase is not reflected in Mixes 6 and 7, so no trend is established and no definite conclusions can be drawn.

6. Hysteresis curves

Hysteresis losses assume some importance in a ferroelectric

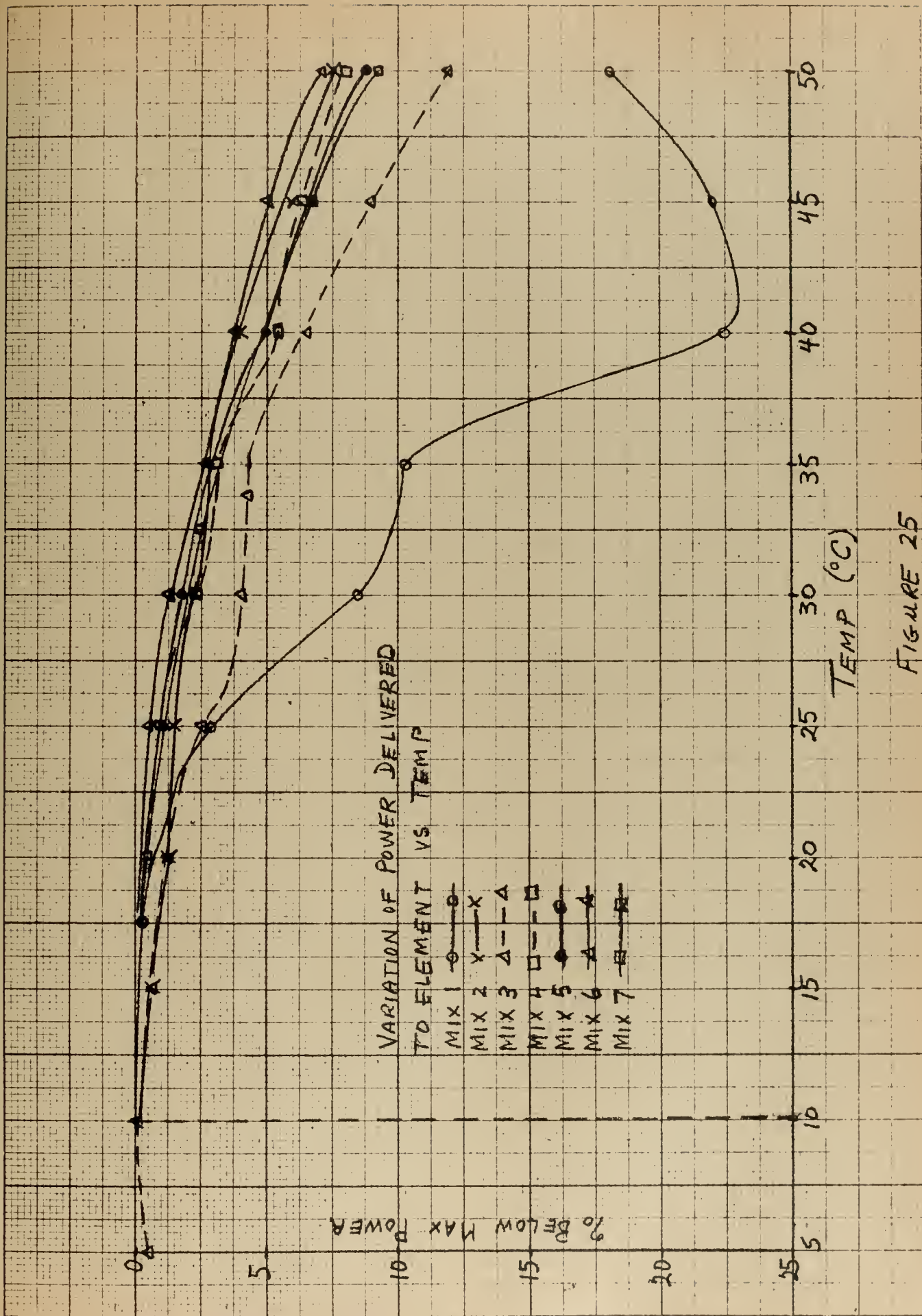


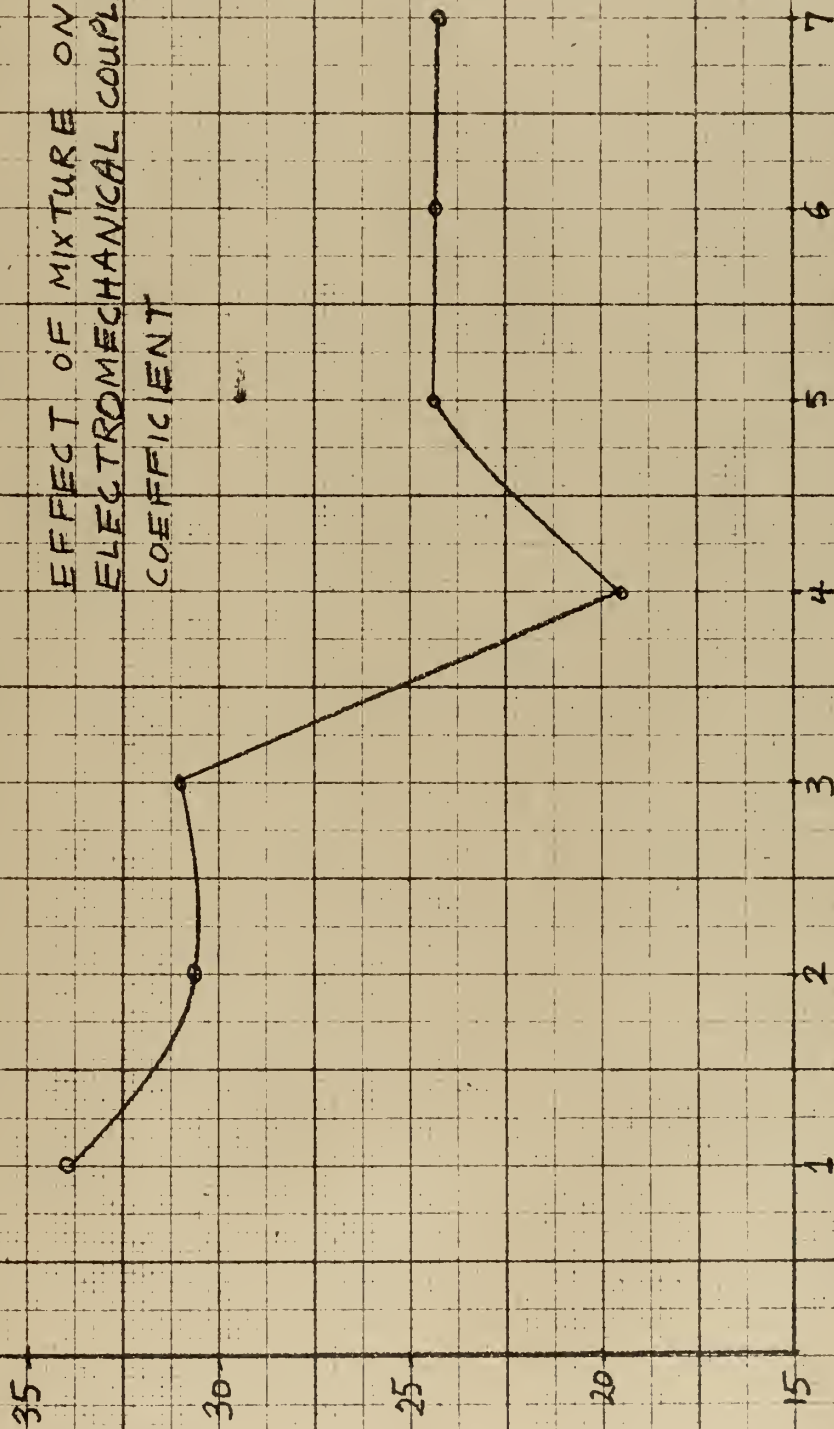
FIGURE 25

EFFECT OF MIXTURE ON
ELECTROMECHANICAL COUPLING
COEFFICIENT

$k \times 100$

MIX NUMBER

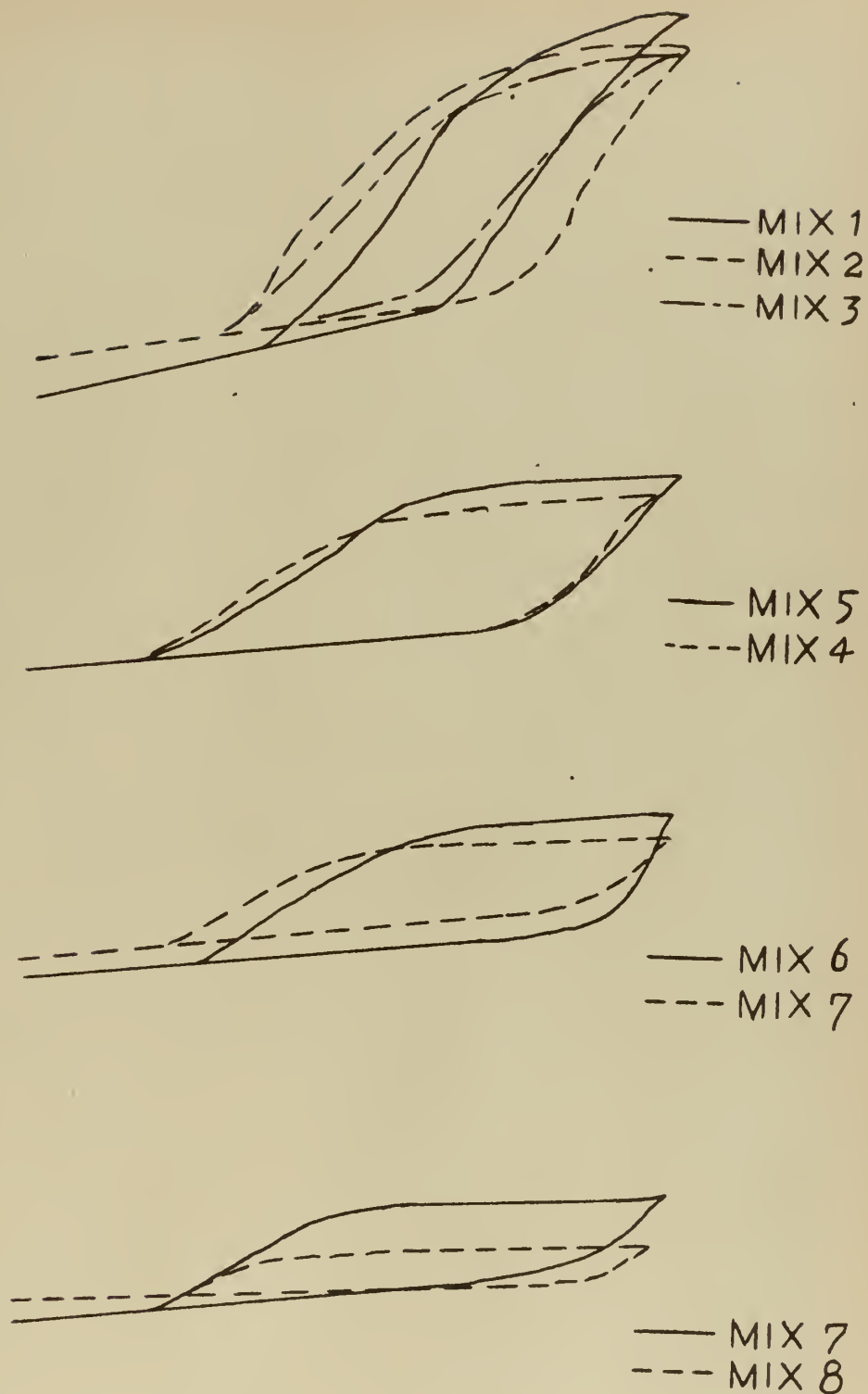
FIGURE 26



ceramic since the end result of hysteresis losses is an internal heating which will at least cause a change in the important "constants" of a transducer and at worst can cause a loss of remanent polarization if heating causes a temperature rise that approaches the Curie point. For that reason hysteresis loops of the mixes with which this paper is concerned were examined with a circuit similar to that of Figure 10. In the hysteresis loops of a polarized ceramic the asymmetry is normal since the polarization in one direction is equal to the sum of the remanent polarization (due to initial d-c polarization) and that due to the a-c driving field while in the opposite direction the polarization is the difference of the two.

An a-c driving voltage of 1600 volts resulting in a field of 12.3 kilovolts per inch across the ceramic elements was used. This driving field was the same for all the elements and is represented by the abscissa of the hysteresis curve. The vertical scale is directly proportional to polarization or electric displacement since the total charge, Q , on the ceramic element is due to dielectric polarization and $D = P = Q/A$ if $A =$ the electrode area.

Items of interest to be noted from the hysteresis loops are (a) the area is proportional to the hysteresis loss, (b) the width of the curve is proportional to coercive force; that is, that field required to reduce the polarization to zero, (c) the vertical height of the curve provides an indication of how easily the particular ceramic can be polarized; that is, since all had the same initial d-c polarization field



HYSTERESIS LOOPS OF E vs D

FIGURE 27

and all are subjected to the same driving field those mixes which do not show a large vertical dimension are less susceptible to being polarized, and (d) the slope of the curve is proportional to the differential dielectric constant.

An examination of Figure 27 brings to light the following facts. Barium titanate with no additives is more susceptible to polarization than any other mix and appears to have less hysteresis loss. This latter fact requires some qualification. A simple comparison of hysteresis loop areas might seem to indicate that the barium titanate loop (Mix 1) encloses a larger area than, say, Mix 7 or Mix 8. However, if these other mixes were subjected to much higher driving and biasing fields in order to bring their polarization to a value approaching that of Mix 1, then the hysteresis losses of these other mixes would far exceed that of the plain barium titanate. The addition of four percent of lead or calcium titanate reduces the polarization only slightly but does increase the hysteresis losses, the loop area of the four percent calcium mixture (Mix 2) exhibiting slightly greater hysteresis losses than does the four percent lead mixture (Mix 3). The addition of larger total percentages of additives further reduces the polarization while it increases the coercivity. Mix 8 which contains 86% of barium titanate and seven percent each of lead and calcium titanate is shown in Figure 27 to further illustrate this point. Furthermore, with a given percent of barium titanate present, the exchange of lead titanate additive for calcium titanate reduces the polarization achievable with a given field strength as

evidenced by examining the loops of Mixes 4 - 7. The slope of the hysteresis loops can be seen to be proportional to dielectric constant although no attempt is made here to measure the dielectric constant by this means due to the unsatisfactory scale of the curves.

CHAPTER V

CONCLUSIONS

Table III represents a compilation of the data presented graphically in Chapter IV. Also included is some data on mixes eight through eleven for which all measurements were not completed.

The first conclusions that may be drawn are that the total amount of additive has some very definite effects upon the properties of the ceramic regardless of the relative amounts of calcium and lead titanates contained therein. The addition of four percent additive reduces the electromechanical coupling coefficient from a value of thirty four percent for Mix 1 to a value of approximately thirty one percent. An increase of additive to eight percent further reduces the electromechanical coupling coefficient to slightly over twenty four percent and a further increase to fourteen percent additive reduces the coupling to somewhat over twenty one percent. The same general behavior may be noted in the change of unpolarized dielectric constant with percent additive, and it appears that a general idea as to the effect of additives upon the coupling coefficient may be gained by examining the change in unpolarized dielectric constant.

The variations of input impedance over the temperature range considered in this paper are considered to have a rather small effect upon the suitability of the ceramic as an under-

water echo ranging transducer. The maximum percentage loss of power delivered to the test element was computed as twenty two and one half percent (or 1.12 decibels) for Mix 1 at 40 degrees. If we assume this variation was encountered in an actual transducer having a source level sufficient to provide a just recognizable echo level at a range of 5000 yards, an application of $E = S - 40 \log r - 2 \alpha r - 2A + T$ indicates a loss in range of 225 yards or 4.5%. This is not significant when the possible echo-to-echo variations in target strength and refraction anomalies are considered. However, in these computations the temperatures considered were temperatures of sea water, and it was tacitly assumed that transducer and surroundings were at the same temperature. This, of course, is not strictly true

TABLE III

(Mix No.	% Ba	% Ca	% Pb	k	K	res	% Power
1	100	0	0	34.1	1910	1.0	22.5
2	96	4	0	30.6	1195	.64	7.5
3	96	0	4	31.0	1395	.483	11.7
4	92	4	4	19.5	853	.30	8.0
5	92	5	3	24.4	934	.415	8.7
6	92	6	2	24.2	916	.46	7.2
7	92	7	1	24.1	971	.485	9.2
8	86	7	7	21.3	675	-	-
9	86	8	6	21.7	677	-	-
10	86	10	4	19.2	667	-	-
11	86	12	2	21.3	636	-	-

in a ceramic transducer; in fact, it may be expected that a ceramic element which may be immersed in castor oil and enclosed in a rubber casing may be quite well insulated thermally from the surrounding medium. Such a transducer subjected to high driving fields may suffer large internal temperature rises which in addition to the detrimental effects upon remanent polarization will also cause wider impedance fluctuations than measured herein. Thus although the data presented here indicates that up to fifty degrees centigrade there is little range loss in this respect, further investigation into internal temperature rises in high power ceramic transducers may indicate that temperature rises well over 50°C may cause significant power losses due to mismatching.

The variations of efficiency at resonance from mix to mix exhibit an interesting behavior and, although the efficiency of all mixes containing additives is below that of plain barium titanate, there appears to be a very definite dependence upon the proportions of the two additives. It is here that the suspected detrimental effects of the lead titanate as an additive become evident, the variation of resonant efficiency following quite closely the variation of the proportion of lead titanate in the ceramic. Mixes 2 and 3 both show a marked decrease in efficiency, the latter mix (containing the lead) exhibiting the largest change. Mix 4 containing a total of eight percent additive (four each of lead and calcium titanates) has the lowest efficiency of all the mixes tested, but now as we proceed, in order, through Mix 7 replacing the lead with calcium

the efficiency rises steadily until the latter mix having twice as much total additive as Mix 3 has very nearly the same efficiency. Since all of these elements were so highly loaded in water, the factor $\frac{D_A - D_W}{D_A}$ in the expression for efficiency at

resonance (Formula 3 - 13) which represents the ratio of mechanical load resistance to total mechanical resistance is very nearly unity in all cases ($R_L \gg R_m$). Thus the variation of efficiency is almost completely determined by the factor $\frac{D_W}{R_{in}}$. A study of the motional impedance circles in water shows that D_W is inversely proportional to the amount of lead titanate while R_{in} is directly proportional; that is both quantities vary in such a way as to make the efficiency inversely proportional to the amount of lead additive. Both of these quantities thus indicate a reduction in the transduction coefficient of ceramics with lead titanate additives.

In the light of these facts it is pertinent to inquire as to what part these additives may play in the manufacture of ceramic transducers. The answer is that these additives have proven themselves desirable in other ways. An examination of the secondary hysteresis loops of Figure 27 shows that additives do increase the coercive force of a ceramic. Examination of the curves of Figures 1 - 7 and 28 shows a much greater temperature stability of dielectric constant with additive, and this stability is extended qualitatively to the temperature stability of other parameters (such as Figure 25). We are then once again faced with the contrariness of nature and forced to compromise

according to the characteristics of most importance to the particular application in mind.

To summarize, the data presented herein proves that the addition of any amount of additive to barium titanate will have a damaging effect upon the electro-acoustic properties important to the use of the ceramic in underwater transducers. This is evidenced by a decrease in electromechanical coupling coefficient and resonant efficiency.

A four percent additive will result in a good increase in temperature stability (up to 50°C) at some loss in efficiency and dielectric constant. Eight percent additive will cause a further loss in efficiency and dielectric constant with very little increased temperature stability. Best compromise between electro-acoustic performance and temperature stability appears to be by limiting the additive to four or five percent. Calcium titanate should be preferred to lead titanate when temperature stability with the best response are the determining factors.

BIBLIOGRAPHY

1. Baerwald, H.G.
Berlin court, D.A. ELECTROMECHANICAL RESPONSE AND DIELECTRIC LOSS OF PREPOLARIZED BARIUM TITANATE UNDER MAINTAINED ELECTRIC BIAS, Part I, Reprinted from The Journal of the Acoustical Society of America, Vol. 25, No. 4, 703-710, July 1953

2. Brush Development
Company GENERAL PROPERTIES OF BRUSH "PIEZOELECTRIC" CERAMIC A, Technical Bulletin E-102, Jan., 1950

3. Brush Development
Company EQUIVALENT CIRCUIT CONSTANTS FOR BRUSH CERAMIC ELEMENTS, Technical Bulletin E-103, Jan., 1950

4. Brush Development
Company BRUSH "PIEZOELECTRIC" CERAMIC ELEMENTS, Technical Bulletin E-105, January 1950

5. Cady, W.G. PIEZOELECTRICITY, 1st Edition, McGraw-Hill, 1946

6. de Brettville, A. OSCILLOGRAPH STUDY OF DIELECTRIC PROPERTIES OF BARIUM TITANATE, Reprinted from The Journal of the American Ceramic Society, Vol. 29, No. 11, 303-307, November 1, 1946

7. Dranetz, A.I.
Howatt, G.N.
Crownover, J.W. BARIUM TITANATES AS CIRCUIT ELEMENTS, Part I, Reprinted from Tele-Tech, April 1949

8. Dranetz, A.I.
Howatt, G.N.
Crownover, J.W. BARIUM TITANATES AS CIRCUIT ELEMENTS, Part II, Reprinted from Tele-Tech, May 1949

9. Dranetz, A.I.
Howatt, G.N.
Crownover, J.W. BARIUM TITANATES AS CIRCUIT ELEMENTS, Part III, Reprinted from Tele-Tech, June 1949

10. Goodman, G. FERROELECTRIC PROPERTIES OF LEAD METANI OBATE, Reprinted from The Journal of the American Ceramic Society, Vol. 36, No. 11, 368-372, November 1953

11. Hueter, T.F.
Bolt, R.H. SONICS, John Wiley and Sons, 1955
12. Hunt, F.V. ELECTROACOUSTICS, John Wiley and Sons, 1954
13. Jaffe, H. ELECTROMECHANICAL PROPERTIES OF TITANATE CERAMICS, Brush Strokes, 1-7, December 1951
14. Kinsler, L.E. INSTRUCTOR'S NOTES, Ph-461, Transducer Theory and Design, USNPS, 1955
15. Kinsler, L.E.
Fry, A.R. FUNDAMENTALS OF ACOUSTICS, John Wiley and Sons, 1950
16. Lane, A.L. BARIUM TITANATE ADMITTANCE-TEMPERATURE CHARACTERISTICS, The Journal of the Acoustical Society of America, Vol. 25, No. 5, 873-878, September 1953
17. Mason, W.P. PIEZOELECTRIC CRYSTALS AND THEIR APPLICATION TO ULTRASONICS, D. Van Nostrand, 1950
18. Mason, W.P. PIEZOELECTRIC OR ELECTROSTRICTIVE EFFECT IN BARIUM TITANATE CERAMICS, Physical Review, Vol. 73, No. 11, 1398, June 1, 1948
19. Metal and Thermit Corporation, New York, N. Y. CERAMIC AND DIELECTRIC PROPERTIES OF THE STANNATES, Technical Data Sheet No. 205, July 1952
20. Metal and Thermit Corporation, New York, N. Y. DIELECTRIC BODIES IN THE QUATERNARY SYSTEM, $\text{BaTiO}_3 - \text{BaSnO}_3 - \text{SrSnO}_3 - \text{CaSnO}_3$, Technical Data Sheet No. 206, July 1952
21. Metal and Thermit Corporation, New York, N.Y. DIELECTRIC BODIES IN METAL STANNATE - BARIUM TITANATE BINARY SYSTEMS, Technical Data Sheet No. 207, November 1953
22. National Bureau of Standards CERAMICS FOR PIEZOELECTRIC TRANSDUCERS, Technical News Bulletin, Vol. 39, No. 11, 149-151, November 1955
23. National Defense Research Committee DESIGN AND CONSTRUCTION OF CRYSTAL TRANSDUCERS, Summary Technical Report of Division 6, Volume 12, 1946

24. Terman, F.E. RADIO ENGINEERING, 3rd Edition,
McGraw-Hill, 1947
25. Von Hippel, A. HIGH DIELECTRIC CONSTANT CERAMICS,
Breckenridge, R.G. Reprinted from Industrial and Engi-
Chesley, F.G. neering Chemistry, 1097-1109, Nov-
Tisza, L. ember 1946

APPENDIX I

DIELECTRIC PROPERTIES OF CERAMIC MIXES

Prior to examining the electromechanical properties of mixes one through seven, the unpolarized dielectric constant was measured as a function of temperature with a view towards determining the Curie point for use in the polarizing technique employed. In addition, similar data was gathered for four other mixes numbered eight through eleven. These latter four mixes all contained eighty six percent barium titanate and the following percentages of calcium titanate and lead titanate respectively; mix eight, seven and seven; mix nine, eight and six; mix ten, ten and four; mix eleven, twelve and two. The plots of the dielectric constant of mixes one through seven as a function of temperature is shown in Figures 1 - 7. Similar data for mixes eight through eleven is shown in Figure 28. In the latter figure values have been plotted up to 110 degrees centigrade only. The effect of lead titanate in raising the Curie temperature is well illustrated, the mixes with the higher percentages of lead showing a "delayed" rise to the peak values of dielectric constant associated with the Curie temperature. There is a consequent greater stability at the lower temperatures. The effect upon the magnitude of the dielectric constant of changing the proportion of lead and calcium titanates is not great, the magnitude depending primarily upon the total percentage of barium titanate in the ceramic.

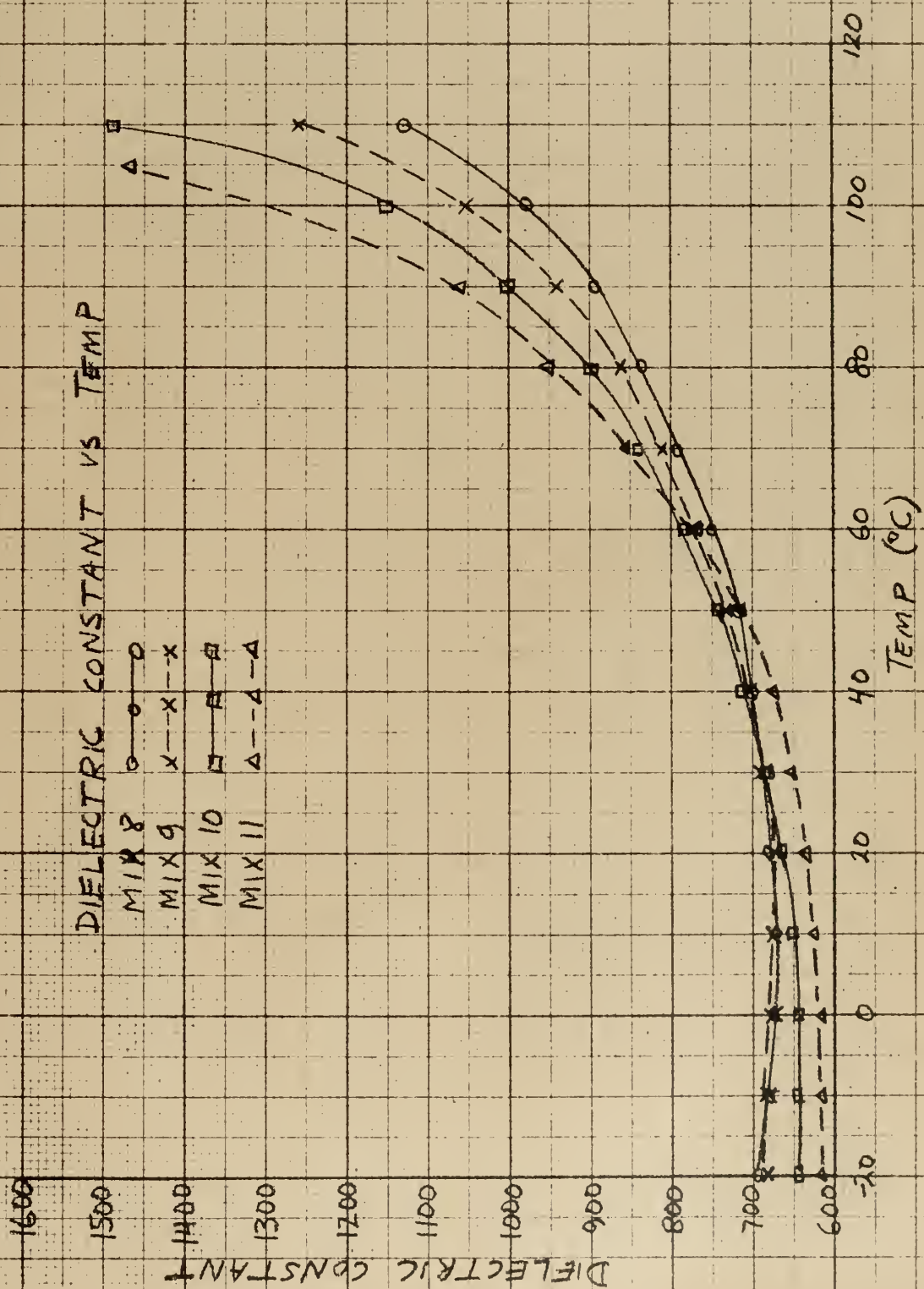


FIGURE 28

This is graphically illustrated in Figure 29 where it is shown that the dielectric constant at room temperature is greatly decreased as the total percentage of additive is increased.

No attempt is made here to further analyze this data. It can be readily seen that different amounts of various additives can control the magnitude and temperature variations of the dielectric constant of ceramic capacitors, and this property has been the subject of considerable research in the electronic and ceramic industry.

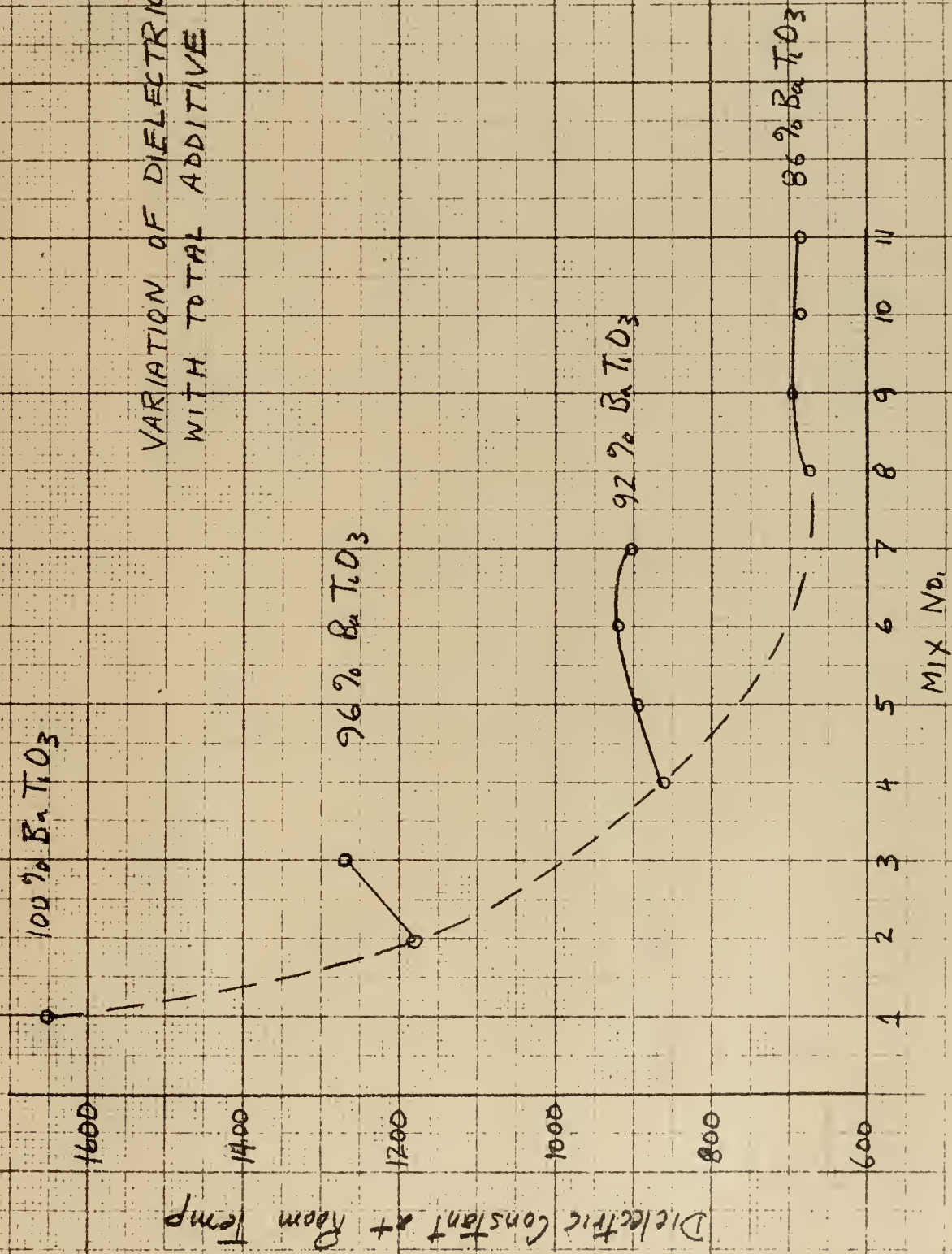


FIGURE 29



Thesis
C512

23983

Clifford

An investigation into
the electro-acoustic
response characteristics
of several mixtures of
the titanates of barium,
calcium and lead.

Thesis
C512

23983

Clifford

An investigation into the
electro-acoustic response
characteristics of several
mixtures of the titanates of
barium, calcium and lead.

thesC512

An investigation into the electro-acoust



3 2768 002 10312 9

DUDLEY KNOX LIBRARY